ORNL-2571
Metallurgy and Ceramics

AN INVESTIGATION OF HOT DUCTILITY OF INCONEL AND INCONEL X

E. A. Pigan

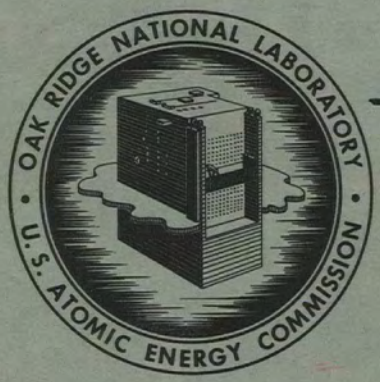

OAK RIDGE NATIONAL LABORATORY
operated by
UNION CARBIDE CORPORATION
for the
U.S. ATOMIC ENERGY COMMISSION

ORNL-2571

Contract No. W-7405-eng-26

METALLURGY DIVISION

AN INVESTIGATION OF HOT DUCTILITY OF INCONEL AND INCONEL X

Edward A. Pigan

DATE ISSUED

SEP 3 1958

OAK RIDGE NATIONAL LABORATORY
Oak Ridge, Tennessee
operated by
UNION CARBIDE CORPORATION
for the
U.S. ATOMIC ENERGY COMMISSION

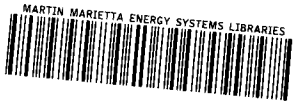

ACKNOWLEDGMENTS

A Thesis submitted to the Faculty of the Department of Metallurgical Engineering, Rensselaer Polytechnic Institute, Troy, New York, June 1956, in partial fulfillment of the requirements for the Degree of Master of Metallurgical Engineering.

This work was performed under Union Carbide Corporation Subcontract No. 371 and was administered under the direction of the Metallurgy Division, Oak Ridge National Laboratory.

The author would like to thank Dr. E. F. Nippes and Dr. W. F. Savage for their guidance, assistance and consideration, without which this work would not have been possible.

TABLE OF CONTENTS

	Page
ABSTRACT	1
INTRODUCTION	2
REVIEW OF LITERATURE	3
OBJECT OF INVESTIGATION	4
EQUIPMENT	5
MATERIAL	15
TESTING PROGRAM	16
RESULTS	23
DISUCSSION	46
SUMMARY AND CONCLUSIONS	48
REFERENCES	49
APPENDIX	51

ABSTRACT

This investigation was undertaken to evaluate the effect of the thermal cycles associated with arc welding in Inconel and Inconel X and to find the cause for the change in properties due to the thermal cycles encountered in arc welding through a metallographic study of the fractured specimens. Modifications on the already built hot ductility time-temperature controller provided for the measurement and recording of the load necessary to fracture a specimen.

Hot ductility and ultimate tensile strength were determined as a function of peak thermal cycles with ductility increasing to a peak value at 2200°F. At temperatures above 2200°F, ductility decreased sharply until at the embrittling temperature (2450°F for Inconel, 2400°F for Inconel X) ductility reached zero for both alloys. The ultimate tensile strength was found to decrease uniformly with the temperature of testing.

For specimens of Inconel fractured on-cooling from 2450°F, the ductility was lowered from the on-heating values but not significantly. The ultimate tensile strength was lowered at the lower temperature of testing but did not vary much from the on-heating values at higher temperatures.

Inconel X, on the other hand, exhibited a drastic loss in ductility when the on-heating values are compared to the ductility of specimens fractured on-cooling from 2400°F. Corresponding to the drastic loss in ductility the ultimate tensile strength was substantially lowered for all test temperatures.

Hot ductility of Inconel fractured on-cooling from 2400°F did not vary significantly from the on-heating values; tensile strength decreased slightly at temperatures below 2000°F. Inconel X specimens exhibited generally lower ductility values when fractured on-cooling from 2350°F than when tested on-heating. Some reduction of tensile strength is noted at lower temperatures but the values compare favorably at the higher temperatures.

The severe loss in ductility of Inconel X is accompanied by gross grain boundary melting. It is possible that melting of the grain boundaries is a factor in hot cracking in the heat-affected zone when Inconel X is welded in large sections.

INTRODUCTION

The need for information about the temperature effect experienced during the welding of alloy steels and super alloys is more acute than ever.

The better creep and corrosion resistance of the higher alloyed steels make them suitable for use in the turbines in the electrical and power fields. Nuclear energy applications have promoted the growth of new uses for known alloys and stirred development for new alloys with special properties.

In jet aircraft, guided missiles, and rockets the higher rates of speeds are causing higher skin temperatures and higher stresses necessitating the use of alloy steels. The big problem facing the manufacturers is the fabrication of these alloys and the effect of the thermal cycle undergone by the material during welding.

In an effort to add information on the time-temperature effects in the welding of these various alloys, the Welding Laboratory at Rensselaer Polytechnic Institute has developed a time-temperature controller that will accurately and consistently expose a specimen to a predetermined thermal cycle. Past work has introduced a means for fracturing the specimen at any desired point. Further modification has led to the attachment of a load cell and oscillograph to provide a means for recording the load data to correlate the ductility studies with tensile strength.

REVIEW OF LITERATURE

Inconel[1] is a corrosion-resistant alloy of essentially 72.0% nickel, 14.0% chromium, 6.0% iron, 1.0% manganese, 0.50% copper, 0.50% silicon, 0.15% carbon and 0.015% sulfur. Nickel contributes in high degree to resistance to corrosion by many organic and inorganic compounds throughout wide ranges of acidity and alkalinity. Chromium confers ability to remain bright under exposure to sulfur compounds in the atmosphere or in other corrosives; it also provides resistance to oxidizing atmospheres at elevated temperatures and to oxidizing conditions in corrosive solutions.

Inconel X is a wrought INCO age-hardened alloy; hardening is obtained by the additions of titanium and aluminum. The alloy was developed to have a low creep rate under high stresses at 1200°F - 1500°F after suitable thermal treatment, and to be highly resistant to chemical corrosion and oxidation. A considerable portion of its high room-temperature strength is retained at temperatures up to 1500°F.

Both alloys are a single phase solid solution when observed under a microscope in the solution treated condition for Inconel X and the wrought forms of Inconel. The aged condition of Inconel X shows up as a fine peppery dispersion throughout the material.

Cross and Freeman[2] in comparing the stress rupture properties of Inconel X, N144, S-590 and S-816 alloys found that Inconel X showed generally superior properties at 1200°F and 1350°F for time periods up to 1000 hours.

Apblett and Pellini[3] compared Inconel X, N155, H U, H W, S-590, EME, 16-25-6 and 19-9DL in their hot cracking tests using 0.650-inch thick material found the Inconel X to be highly crack resistant.

OBJECT OF INVESTIGATION

The object of the investigation was:

1. To study the effect of the rapid time-temperature cycles associated with arc welding on the hot ductility of Inconel and Inconel X.
2. Once the effect was determined, to endeavor to find the cause for the change in properties due to the rapid time-temperature cycles encountered in arc welding through a metallographic study of the fractured specimens.

EQUIPMENT

For this investigation the high speed time-temperature controller already constructed and used for the determination of the hot ductility of other alloys[4,5] at Rensselaer Polytechnic Institute was further modified to provide for the measurement and recording of the applied load necessary to fracture a specimen.

A generalized description of equipment and method of operation is included below. Figure 2 is a photograph of the actual testing apparatus.

The specimen is mounted in one movable and one fixed jaw modeled after Templin grips used in tensile machines such that a tensile stress will produce good mechanical and electrical contact between the specimen and the jaws. Besides holding the specimen during testing, the jaws served to complete part of the secondary loop of a 38 KVA welding transformer to furnish the heating current, and to also provide a means for producing the required cooling rates in the specimens. The jaws with a specimen during a heating cycle is shown in Figure 3.

A fine wire (0.010 in chromel-alumel duplex) open circuit thermocouple is percussion welded to the specimen at the center of the free length. This junction supplied a voltage E_1 proportional to the temperature of the specimen which is connected in series with a voltage E_2 from the specially designed cam-operated slide-wire potentiometer. Any desired thermal cycle can be reproduced in a specimen by inserting a cam duplicating the desired cycle. As shown in schematic diagram of Figure 1 by connecting E_1 from the thermocouple with E_2 from the potentiometer in a series bucking arrangement, an error signal E_3 is produced which is proportional to the difference between the desired temperature and the instantaneous temperature in the specimen. The polarity of E_3 is dependent on whether the temperature of the specimen is higher or lower than the desired value as determined from the cam-controlled potentiometer. This error signal is fed into a high-gain amplifier that will amplify the signal by 500,000 times to E_4, which is mixed with a D. C. bias supply and fed to the control thyratrons. These thyratrons in turn fire the ignition contactor in the primary of the 38 KVA welding transformer.

Whenever the specimen is below the instantaneous value of the potentiometer, the resulting error signal E_3 will cause the control to initiate the thyratrons

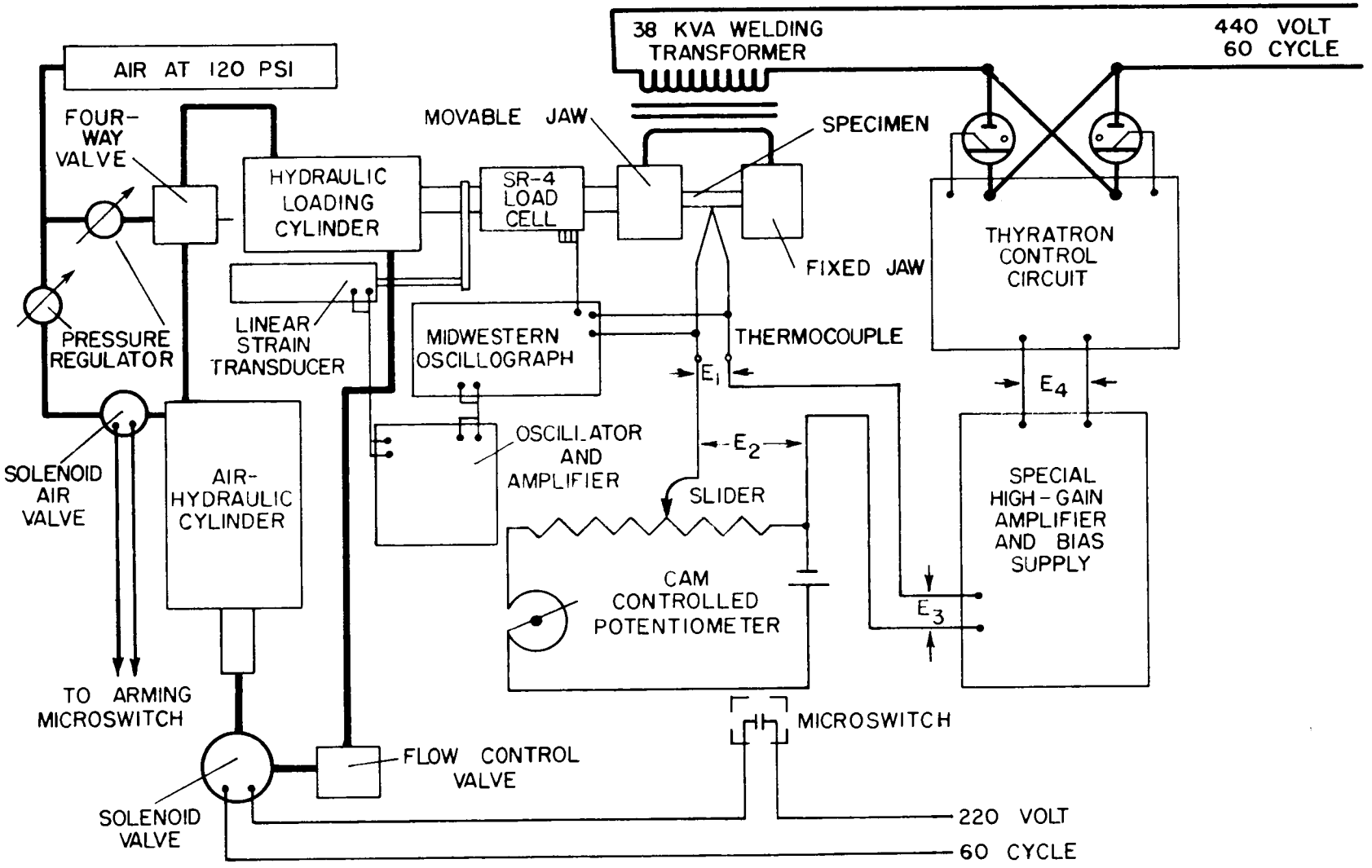

SCHEMATIC DIAGRAM OF HOT DUCTILITY EQUIPMENT

Fig. 1

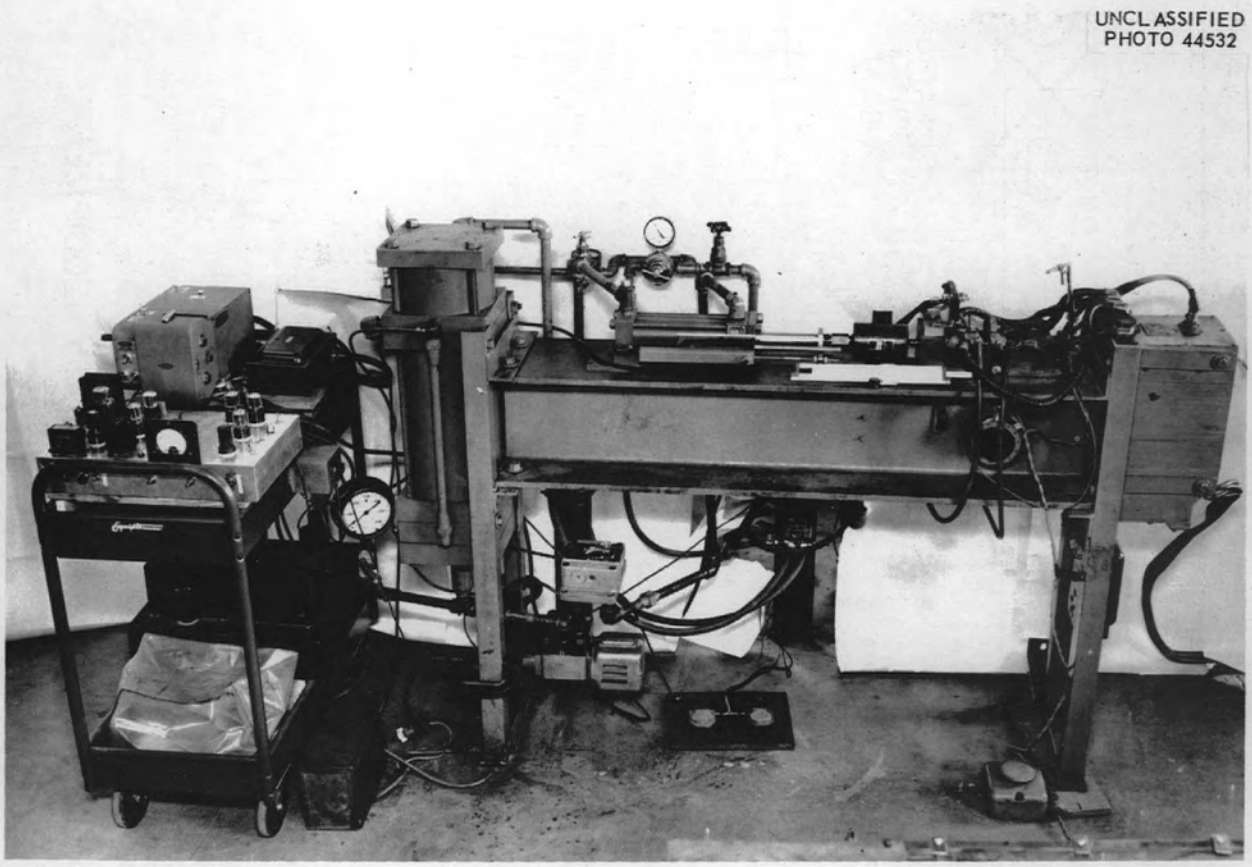

Hot Ductility Testing Apparatus

Fig. 2

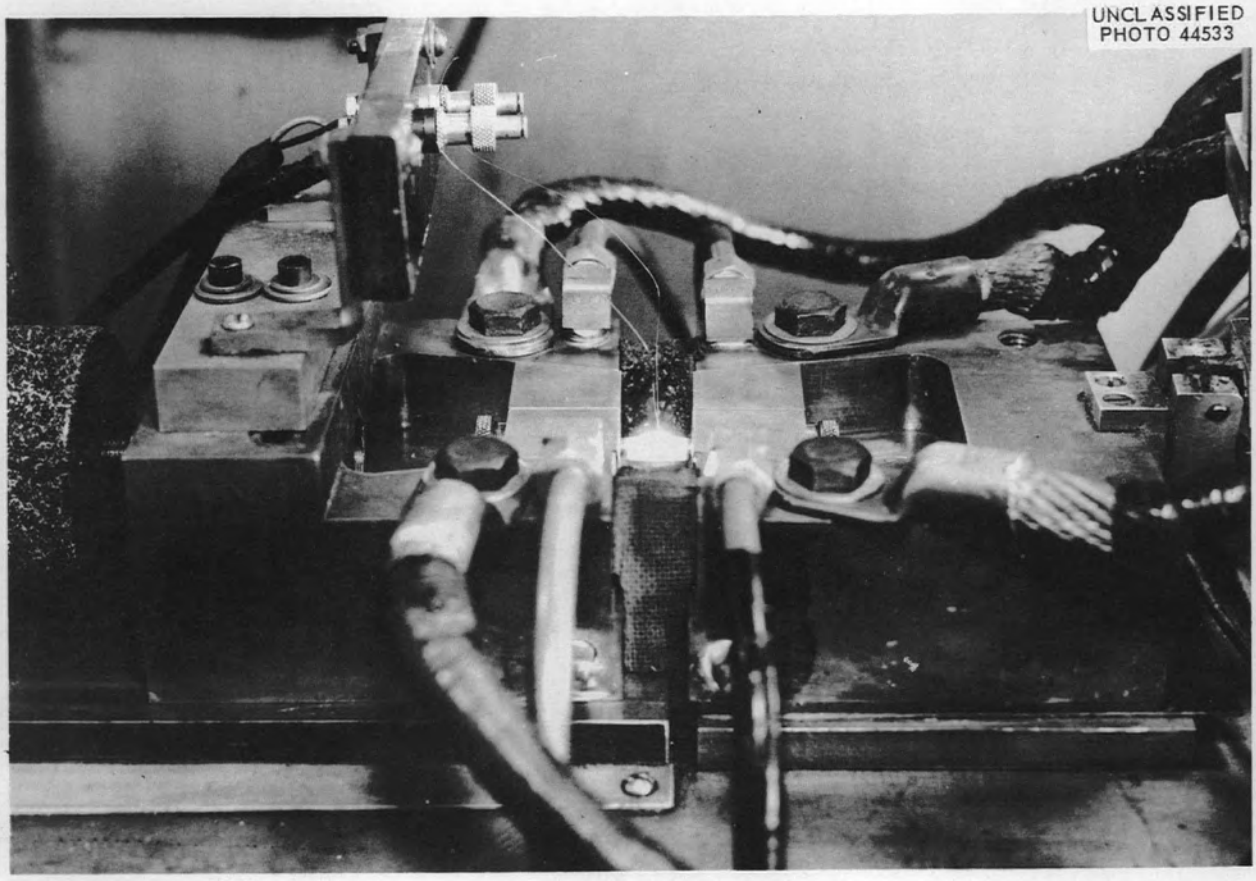

Specimen Clamped in Jaws While Heating

Fig. 3

and the transformer supplying heat to the specimen by resistance heating increasing the E_1 voltage until it balances E_2. In effect the error signal is zero and the temperature of the specimen is at the desired instantaneous value.

Should the temperature of the specimen be above the desired value, then the error signal is such that it will not allow current to flow in the specimen and thus cooling will take place through the water-cooled jaws reducing the specimen temperature to the required value. In this manner the instantaneous temperature of the specimen is controlled to plus or minus 15° as determined in previous work[5].

LOADING DEVICE FOR APPLYING LOAD TO SPECIMEN

The loading device consists of a movable jaw connected to a SR 4 load cell which in turn is connected to a 2 1/2-inch diameter hydraulic cylinder. Hydraulic oil at high pressure is admitted to the hydraulic cylinder through a flow control valve to load the specimen to failure. The flow control valve can be adjusted to allow the loading of the specimen at any desired rate between 0.10 to 21.0 i.p.s. In this investigation a rate of 1.0 i.p.s. was used.

An air hydraulic cylinder which converted air pressure at 100 psi to an oil pressure of 300 psi was used to provide the high pressure fluid to fracture the specimen. The piston was actuated by two microswitches mounted on the cam-operated potentiometer. The adjustable microswitches made it possible to load the specimen at any desired point in the heating or cooling cycle.

One microswitch served to initiate the solenoid air-control valve to the air-hydraulic cylinder while the second microswitch opened the oil valve to supply the force to fracture the specimen. The air microswitch was initiated in advance of the oil switch to prevent any lag in building up the oil pressure when the breaking point was reached.

INSTRUMENTATION FOR MEASURING AND RECORDING THE LOAD AND STRAIN DATA

In order to measure the load necessary to fracture a specimen either a 2000 pound or a 10,000 pound SR 4 load cell was connected between the hydraulic piston and the movable jaw. The load cell consisted of a strain gage bridge which was connected to a 6 volt D. C. source and fed into a galvanometer of the recording oscillograph. The application of a load would unbalance the bridge of the load cell and the amount of unbalance is a measure of the load permanently recorded on the film of the oscillograph. The film of the oscillograph was actuated by a third microswitch on the cam-operated potentiometer. The microswitch was adjusted to initiate the film just before the application of the

fracturing load with the filming interval set on a time delay switch to allow enough time for recording the load for fracture. Strain data were obtained by mounting a linear strain transducer on the chassis of the testing apparatus shown to the left of the slide rule in Figure 2. The transducer essentially consists of coils with a moving paramagnetic shaft connected to the piston. The impedance of the coil will depend on the position of the paramagnetic shaft in the two coils. A signal is obtained from the coils depending on the amount of unbalance applied and fed into a galvanometer of the Midwestern oscillograph providing a permanent record of the strain.

The strain transducer power source amplifier and Midwestern oscillograph are shown in Fig. 2 in the left of the photo.

MASTER CAM

The master cams to develop the various thermal cycles were determined from temperature measurements in 1 1/2-in. stainless steel plate[6]. The heating and cooling rates were those experienced in the heat-affected zones of a weld made with 70,000 joules per inch for 1 1/2-in. plate at the indicated distances from the weld centerline shown in Figure 4. A series of cams were used to study the weld thermal cycles for peak values of 1500°F to 2500°F.

SPECIMENS

The size of the specimen is 4.5-in. long with a 0.250-in. diameter +0.001-0.000. In order to keep a constant free length, the stop nuts were tightened to fixed positions on a pattern and transferred to the jaws. After positioning in the jaws, a slight preload was temporarily applied to insure good electrical and mechanical contact between specimen and the jaws.

THERMOCOUPLE

An open circuit chromel alumel duplex thermocouple was used to measure the temperature of the specimen and to provide the E_1 voltage in Fig. 1. One thermocouple was used for each sample; each wire of 0.010 in. (chromel alumel duplex) was individually percussion welded to the center of the free length approximately 1/16 of an inch apart, as shown in Fig. 5. This was facilitated by mounting the welding arm of a capacitator discharge welder on the stationary jaw serving to keep the position of the thermocouple constant for all specimens.

A low-temperature check run at 500°F preceeded each actual thermal cycle run in order to check on the thermocouple specimen weld.

The details of preliminary and actual testing procedure and calibration of the equipment are included in the appendix to this report.

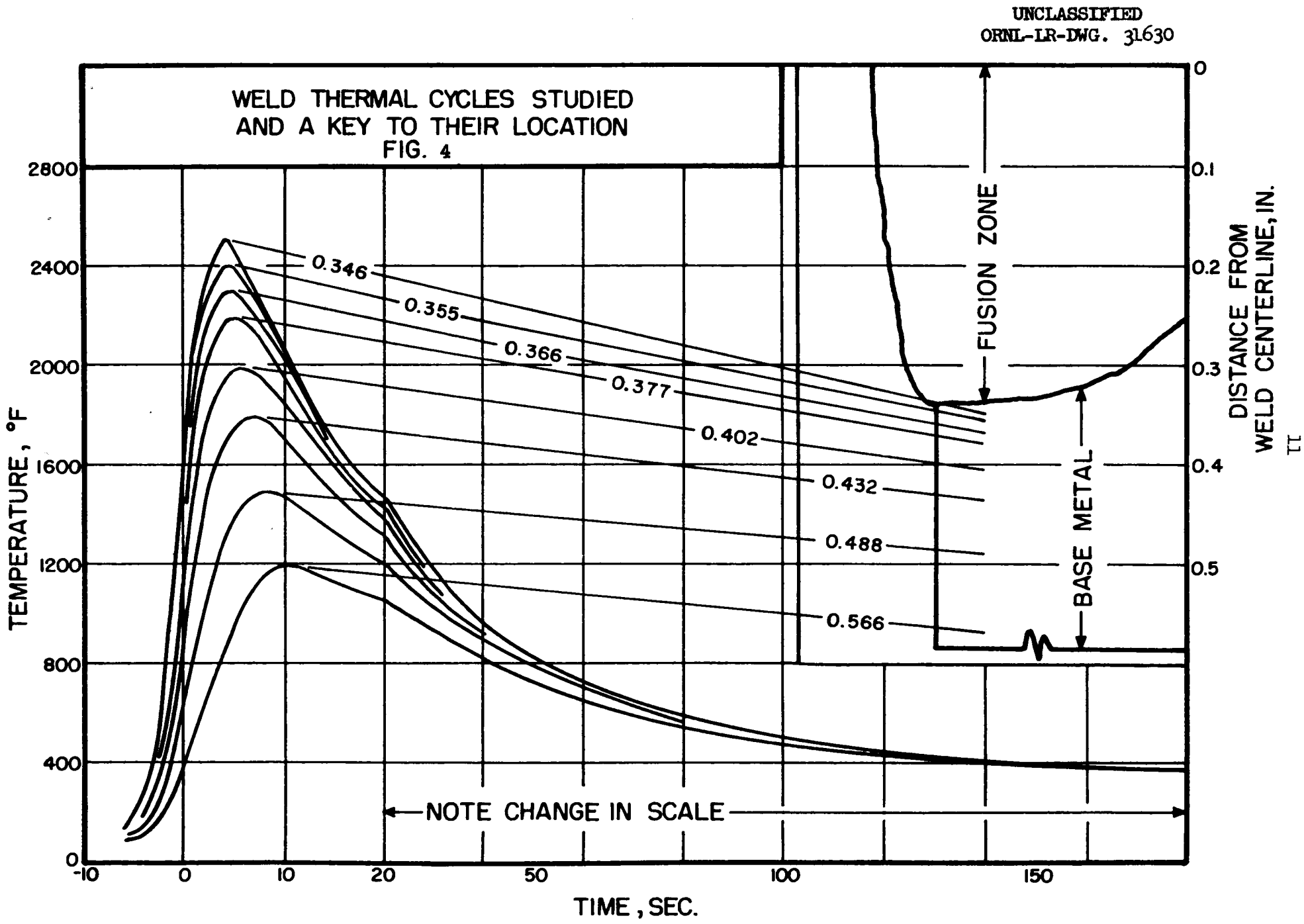
UNCLASSIFIED
ORNL-LR-DWG. 31630
WELD THERMAL CYCLES STUDIED
AND A KEY TO THEIR LOCATION
FIG. 4
TEMPERATURE, °F
2800
2400
2000
1600
1200
800
400
0
0.346
0.355
0.366
0.377
0.402
0.432
0.488
0.566
FUSION ZONE
BASE METAL
DISTANCE FROM
WELD CENTERLINE, IN.
0
0.1
0.2
0.3
0.4
0.5
NOTE CHANGE IN SCALE
-10
0
10
20
50
100
150
TIME, SEC.

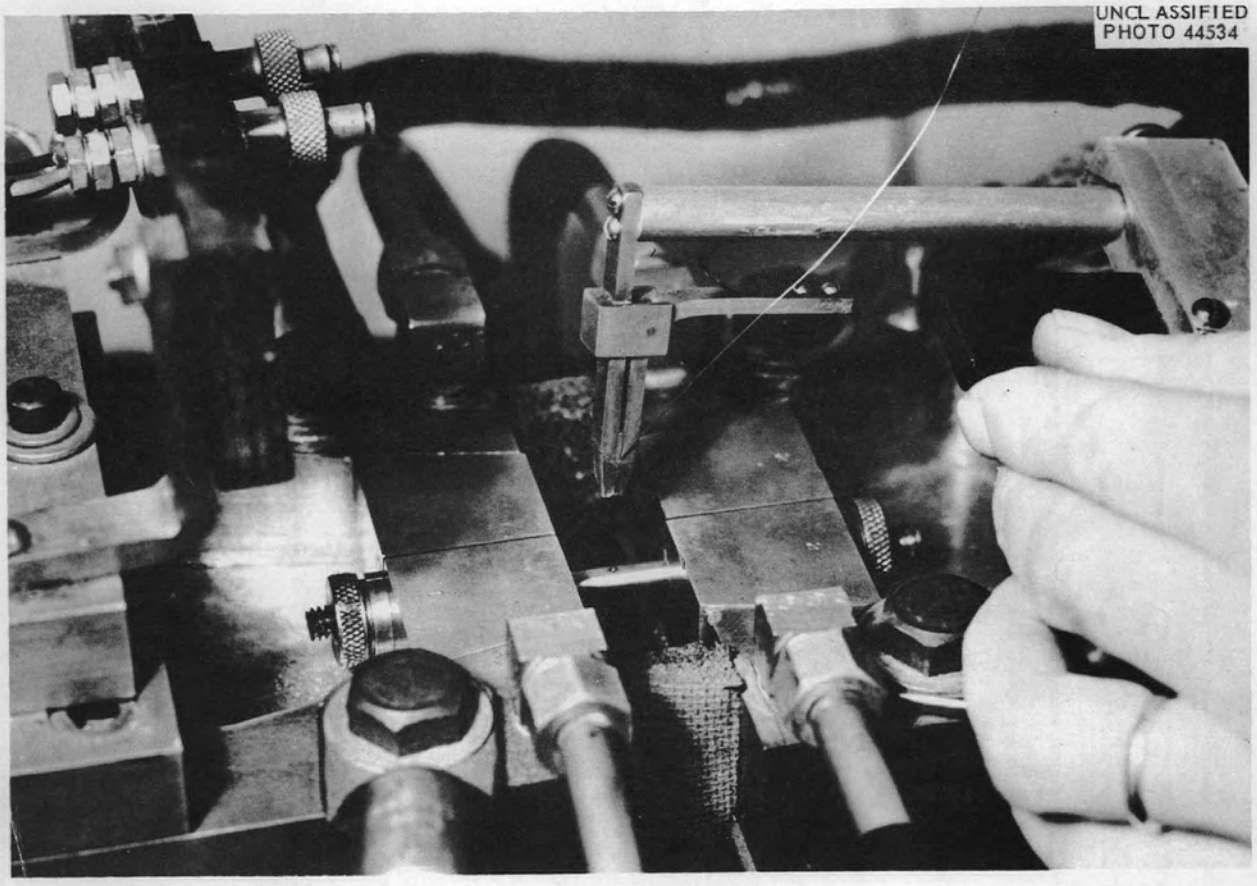

Thermocouple Wire Being Welded to the Specimen

Fig. 5

VALIDITY OF SPECIMENS

While each test run was in progress, a permanent record of the firing pattern was made on a Brush self-inking oscillograph shown in Fig. 6. The load, temperature, and strain was recorded on the Midwestern oscillograph shown in Fig. _.

The validity of specimens was judged on the basis of:

1. The firing pattern recorded on Brush oscillograph during actual test run.
2. The temperature recorded on oscillograph at fracture.

A sample was considered satisfactory if both of the above criteria were in agreement with proper operating conditions.

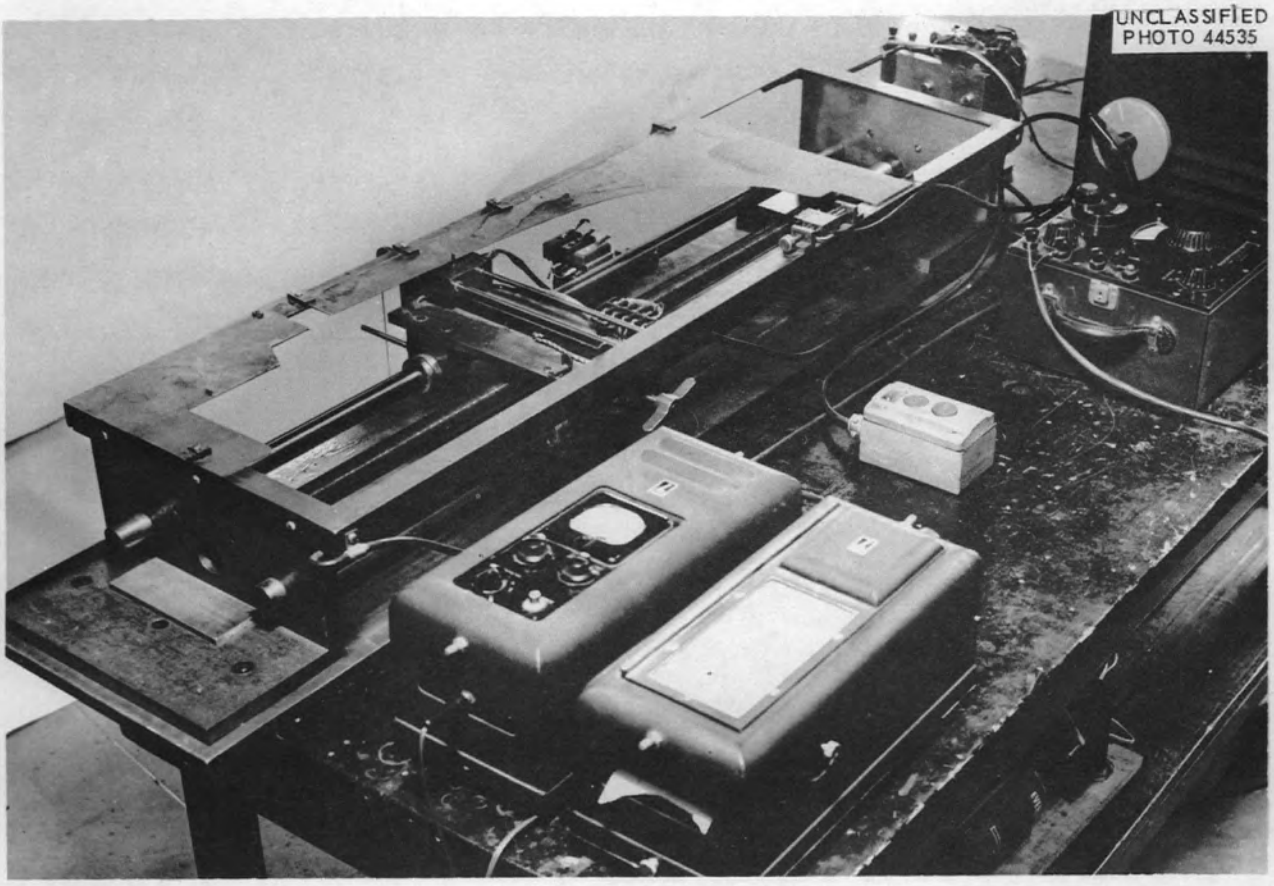

Brush Oscillograph and Cam-Potentiometer

Fig. 6

MATERIAL

Two materials were used in this investigation. The first was Inconel, Heat No. 4089, with a chemical composition of:

Element	Percent	Element	Percent
C	0.09	Ni	76.01
Mn	0.24	Cu	0.13
Si	0.30	Fe	7.40
Cr	15.80	S	0.007

As received Tensile Strength 109,000 psi.

The other was Inconel X, Heat No. 4873, with a chemical composition of:

Element	Percent	Element	Percent
C	0.03	Fe	6.43
Mn	0.53	S	0.007
Si	0.19	Ta Cb	0.89
Cr	14.86	Ti	2.36
Ni	74.04	Ac	0.62

As received Tensile Strength 125,000 psi. according to certificate of analysis.

TESTING PROGRAM

THERMAL CYCLES INVESTIGATED

In order to determine the effect of the various thermal cycles on hot ductility, a series of specimens were fractured at the indicated temperatures of Table I for Inconel and Table II for Inconel X. Each temperature is a peak value of a curve given in Fig. 4. Increasingly higher thermal cycles were used until a point of zero ductility was obtained. The cycle that produced a fracture with zero ductility was considered the damaging thermal cycle.

To determine the extent of damage due to exposure to this damaging thermal cycle, a series of specimens were fractured on cooling from the damaging thermal cycle. These conditions are given in Tables 3 and 4 for Inconel and Inconel X, respectively. A third series of specimens were fractured on cooling from a thermal cycle 50°F below the damaging thermal cycle; these conditions are given in Tables 5 and 6 for Inconel and Inconel X.

TABLE I

CONDITIONS STUDIED TO EVALUATE THE EFFECT OF THERMAL CYCLES NEAR AN ARC WELD ON THE HOT DUCTILITY OF INCONEL, HEAT NO. 4089

Specimens fractured at the various temperatures along the heating portion of the curves of Fig. 4.

Temperature of Test °F	No. of Specimens Tested to Failure	No. of Specimens Prepared for Metallographic Study
1500	6	1
1800	3	1
2000	3	1
2200	3	1
2300	4	1
2350	2	1
2400	3	1
2450	3	1
2500	2	1

TABLE II

CONDITIONS STUDIED TO EVALUATE THE EFFECT OF THERMAL CYCLES NEAR AN ARC WELD ON THE HOT DUCTILITY OF INCONEL X, HEAT NO. 4873

Specimens fractured at the various temperatures along the heating portion of the curves of Fig. 4.

Temperature of Test	No. of Specimens Tested to Failure	No. of Specimens Prepared for Metallographic Study
1500	6	1
1800	4	1
2000	6	1
2200	3	1
2300	3	1
2350	3	1
2400	3	1

TABLE III

CONDITIONS STUDIED TO EVALUATE THE EFFECT OF THERMAL CYCLES NEAR AN ARC WELD ON THE HOT DUCTILITY OF INCONEL, HEAT NO. 4089

Specimens fractured at various indicated temperatures along the cooling portion of the uppermost curve of Fig. 4. (i.e., after heating to a peak temperature of 2450°F)

Temperature of Test °F	No. of Specimens Tested to Failure	No. of Specimens Prepared for Metallographic Study
1800	2	1
2000	3	1
2200	3	1
2300	3	1

TABLE IV

CONDITIONS STUDIED TO EVALUATE THE EFFECT OF THERMAL CYCLES NEAR AN ARC WELD ON THE HOT DUCTILITY OF INCONEL X, HEAT NO. 4873

Specimens fractured at the various indicated temperatures along the cooling portion of the curve after heating to a peak temperature of 2400°F.

Temperature of Test °F	No. of Specimens Tested to Failure	No. of Specimens Prepared for Metallographic Study
1500	6	1
1800	3	1
2000	3	1
2200	3	1
2300	3	1

TABLE V

CONDITIONS STUDIED TO EVALUATE THE EFFECT OF THERMAL CYCLES NEAR AN ARC WELD ON THE HOT DUCTILITY OF INCONEL, HEAT NO. 4089

Specimens fractured at the various indicated temperatures upon cooling from a peak temperature of 2400°F.

Temperature of Test °F	No. of Specimens Tested to Failure	No. of Specimens Prepared for Metallographic Study
1500	3	1
1800	3	1
2000	3	1
2200	3	1
2300	3	1

TABLE VI

CONDITIONS STUDIED TO EVALUATE THE EFFECT OF THERMAL CYCLES NEAR AN ARC WELD ON THE HOT DUCTILITY OF INCONEL X, HEAT NO. 4873.

Specimens fractured at various temperatures along the cooling portion of the thermal cycle with peak temperature of 2350°F, Fig. 4.

Temperature of Test	No. of Specimens Tested to Failure	No. of Specimens Prepared for Metallographic Study
1500	3	1
1800	3	1
2000	3	1
2200	3	1
2300	3	1

RESULTS

REDUCTION IN AREA AND ULTIMATE TENSILE STRENGTH MEASUREMENTS

The results on hot ductility due to the various thermal cycles in Fig. 4 are given in Tables 7, 9, and 11 for per cent reduction in area and ultimate tensile strength for tests on Inconel. Tables 8, 10, and 12 contain the same data for Inconel X. Figures 7 and 11 are summaries of the reduction in area and ultimate tensile strength, respectively, for specimens of Inconel fractured on heating to various peak temperatures as indicated in Table 7. Table 8 is summarized in Figs. 13 and 16 for the same conditions using Inconel X.

For both Inconel and Inconel X, the ductility can be observed to increase as the testing temperature is increased until a peak value at 2200°F is reached. Above this temperature the fracture rapidly becomes more brittle until a point is reached where the ductility reaches zero at 2400°F for Inconel X and at 2450°F for Inconel.

Corresponding to the increase of ductility as the temperature of testing is increasing, the ultimate tensile strength decreases for both Inconel and Inconel X as illustrated in Figs. 11 and 16. Even above 2200°F where ductility begins to fall, the strength continues to decrease until it is only a small value at the temperature which results in zero ductility.

The results of heating to the damaging temperature (2450°F for Inconel, 2400°F for Inconel X) and testing on the cooling portion of the cycle are given in Tables 9 and 10 for Inconel and Inconel X, respectively. The summaries of per cent reduction in areas and ultimate tensile strengths are given in Figs. 10 and 9 for Inconel and Figs. 14 and 17 for Inconel X.

The hot ductility curve obtained on-cooling for Inconel, as shown for Fig. 10, while generally lower than the on-heating curve, Fig. 7, still retains its general characteristic shape of an increase to a maximum at 2200°F and a rapid decrease to 2450°F. At the higher testing temperatures very little difference can be discerned between the on-heating tensile values, Fig. 11 and the on-cooling values in Fig. 9. The tensile strength is lowered at the lower temperatures but not to a large extent (from 41,800 psi on-heating to 35,000 psi on-cooling at 1800°F.)

Inconel X, on the other hand, shows a drastic loss in ductility on-cooling. As may be noted by comparing Figs. 13 and 14, the ductility does not at any

TABLE VII

RESULT OF REDUCTION IN AREA AND ULTIMATE TENSILE STRENGTH MEASUREMENTS MADE ON INCONEL HEAT NO. 4089

Specimens fractured at the indicated temperatures along the heating portion of the curve Fig. 4.

Temperature of Test °F	Per Cent Reduction in Area	Average Value	Ultimate Tensile Strength psi	Average Value
1500	69.5			
	69.3			
	69.5			
	69.9		66,400	
	70.9		66,600	66,500
	70.4	69.9	66,600	
1800	90.3		40,400	
	91.0		42,900	41,800
	90.3	90.5	41,900	
2000	98.0		24,200	
	98.5	98.3	24,200	24,200
	98.4		24,200	
2200	99.3		14,800	
	99.4	99.4	16,000	15,300
	99.5		15,100	
2300	94.8		13,300	
	81.3		12,500	
	87.6		13,000	
	84.4	87.0	12,700	12,800
2350	17.2		8,490	
	21.0	19.1	8,780	8,640
2400	1.0		3,230	
	6.6		315	

TABLE VII (Cont'd)

Temperature of Test °F	Percent Reduction in Area	Average Value	Ultimate Tensile Strength psi	Average Value
	7.0	4.9	404	1,310
2450	0.5		500	
	0.0		500	
	0.6	0.3	500	500
2500	0.0		2,520	
	0.0		4,040	3,270

TABLE VIII

RESULT OF REDUCTION IN AREA AND ULTIMATE TENSILE STRENGTH MEASUREMENTS MADE ON INCONEL X HEAT NO. 4873

Specimens fractured at the indicated temperatures along the heating portion of the curve, Fig. 4 on heating.

Temperature of Test °F	Per Cent Reduction in Area	Average Value	Ultimate Tensile Strength psi	Average Value
1500	53.3		83,800	
	52.8		85,800	
	52.7		82,800	
	54.0		86,900	
	53.3		85,400	
	53.2	53.2	85,400	85,000
1800	79.7		54,500	
	79.4		56,500	
	79.2		55,000	
	79.2	79.4	55,000	55,300
2000	93.6			
	93.4			
	92.7			
	91.8		34,800	
	93.7		35,800	
	93.0		35,800	
	91.6	92.8	33,800	34,900
2200	97.7		18,000	
	97.6		18,700	
	95.5	96.9	17,600	18,100
2300	79.2		15,400	
	85.5		14,700	
	80.8	81.8	14,300	14,800

TABLE IX

RESULT OF REDUCTION IN AREA AND ULTIMATE TENSILE STRENGTH MEASUREMENTS MADE ON INCONEL HEAT NO. 4089

Specimens fractured at the indicated temperatures along the cooling portion of the curve Fig. 4 after heating to a peak temperature of 2450°F.

Temperature of Test °F	Per Cent Reduction in Area	Average Value	Ultimate Tensile Strength psi	Average Value
1800	50.2		35,200	
	64.7	57.4	34,900	35,000
2000	67.8		22,800	
	68.5		22,300	
	67.6	68.0	21,200	22,100
2200	75.8		14,300	
	79.8		14,600	
	80.1	78.6	14,700	14,600
2300	16.6		9,200	
	20.7		8,900	
	8.2	15.2	7,000	8,400

TABLE X

RESULTS OF REDUCTION IN AREA AND ULTIMATE TENSILE STRENGTH MEASUREMENTS MADE ON INCONEL X HEAT NO. 4873

Specimens fractured at the indicated temperature along the cooling portion of the curve Fig. 4 after heating to a peak temperature of 2400°F.

Temperature of Test °F	Per Cent Reduction in Area	Average Value	Ultimate Tensile Strength psi	Average Value
1500	27.8		56,500	
	26.2		55,000	
	27.8		55,600	55,700
	23.5			
	24.5			
	24.7	25.8		
1800	26.2		42,900	
	38.5		48,000	
	13.0	25.9	33,400	41,400
2000	28.7		24,200	
	28.0		24,600	
	38.4	31.7	26,400	25,200
2200	15.0		13,900	
	1.4		13,600	
	6.8	7.7	14,000	13,900
2300	0.0			
	0.0	0.0		
	0.0			

TABLE XI

RESULTS OF REDUCTION IN AREA AND ULTIMATE TENSILE STRENGTH MEASUREMENTS MADE ON INCONEL HEAT NO. 4089

Specimens fractured at the indicated temperatures along the cooling portion of the curve Fig. 4 after heating to a peak temperature of 2400°F.

Temperature of Test °F	Per Cent Reduction in Area	Average Value	Ultimate Tensile Strength psi	Average Value
1500	58.3		57,500	
	58.9		57,500	
	57.0	58.1	55,600	56,800
1800	84.8		33,600	
	85.6		34,600	
	81.5	84.0	33,600	33,900
2000	83.4		19,800	
	91.4		20,300	
	96.5	90.4	22,600	20,900
2200	94.7		12,100	
	96.8		12,100	
	95.0	95.8	12,100	12,100
2300	41.9		14,200	
	49.3		15,400	
	41.5	44.2	14,800	14,800

TABLE XII

RESULTS OF REDUCTION IN AREA AND ULTIMATE TENSILE STRENGTH MEASUREMENTS MADE ON INCONEL X HEAT NO. 4873

Specimens fractured at the indicated temperature along the cooling portion of the curve Fig. 4 after heating to a peak temperature of 2350°F.

Temperature of Test °F	Per Cent Reduction in Area	Average Value	Ultimate Tensile Strength(psi)	Average Value
1500	31.2		61,600	
	26.2		73,200	
	29.6	29.0	77,800	70,800
1800	45.4		55,000	
	49.5		56,500	
	51.8	48.9	58,100	56,500
2000	79.7			
	80.0		36,900	
	79.7	79.8	39,900	38,400
2200	82.3		24,800	
	81.2		23,200	
	86.5	83.3	22,700	23,600
2300	90.2		14,100	
	78.9		14,100	
	53.9	74.3	13,800	14,000

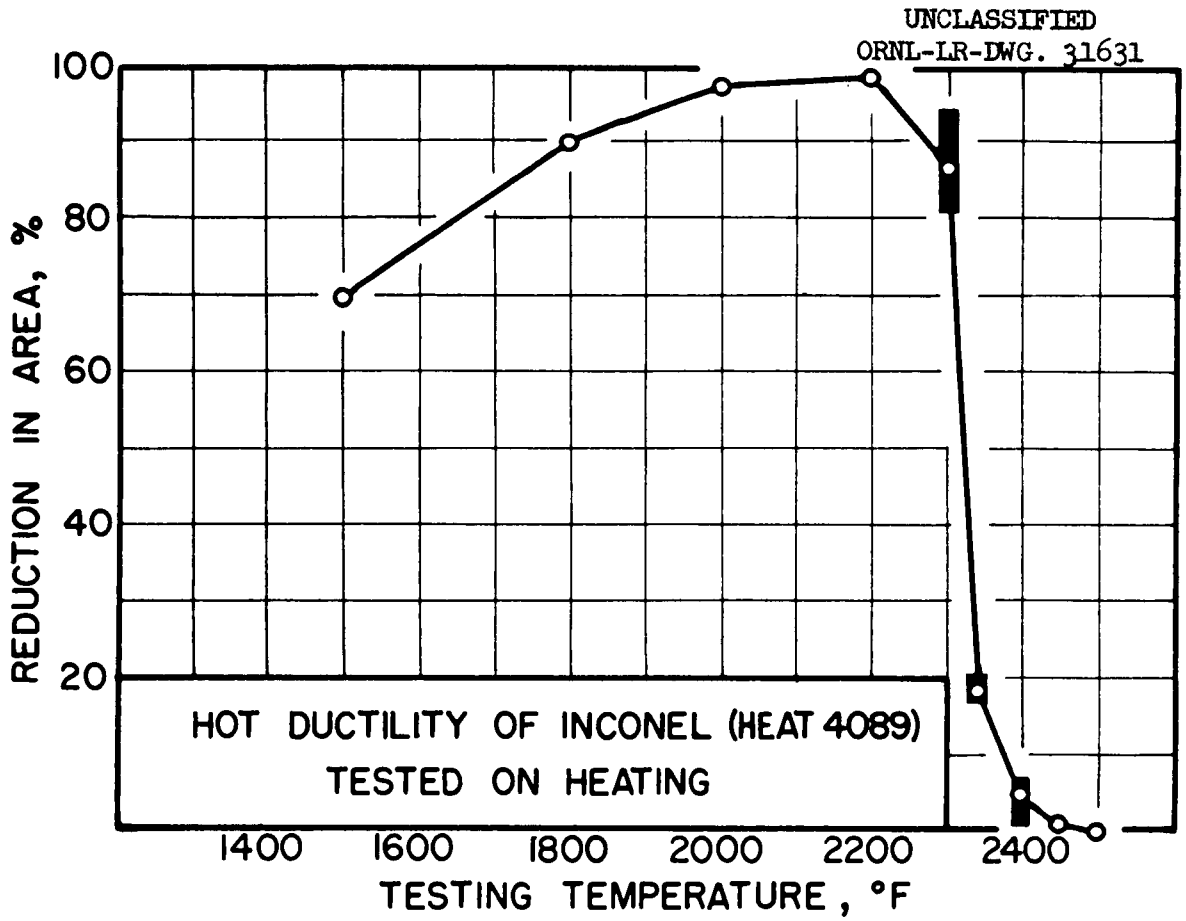
UNCLASSIFIED
ORNL-LR-DWG. 31631
100
80
60
40
20
REDUCTION IN AREA, %
HOT DUCTILITY OF INCONEL (HEAT 4089)
TESTED ON HEATING
1400
1600
1800
2000
2200
2400
TESTING TEMPERATURE, °F

Fig. 7

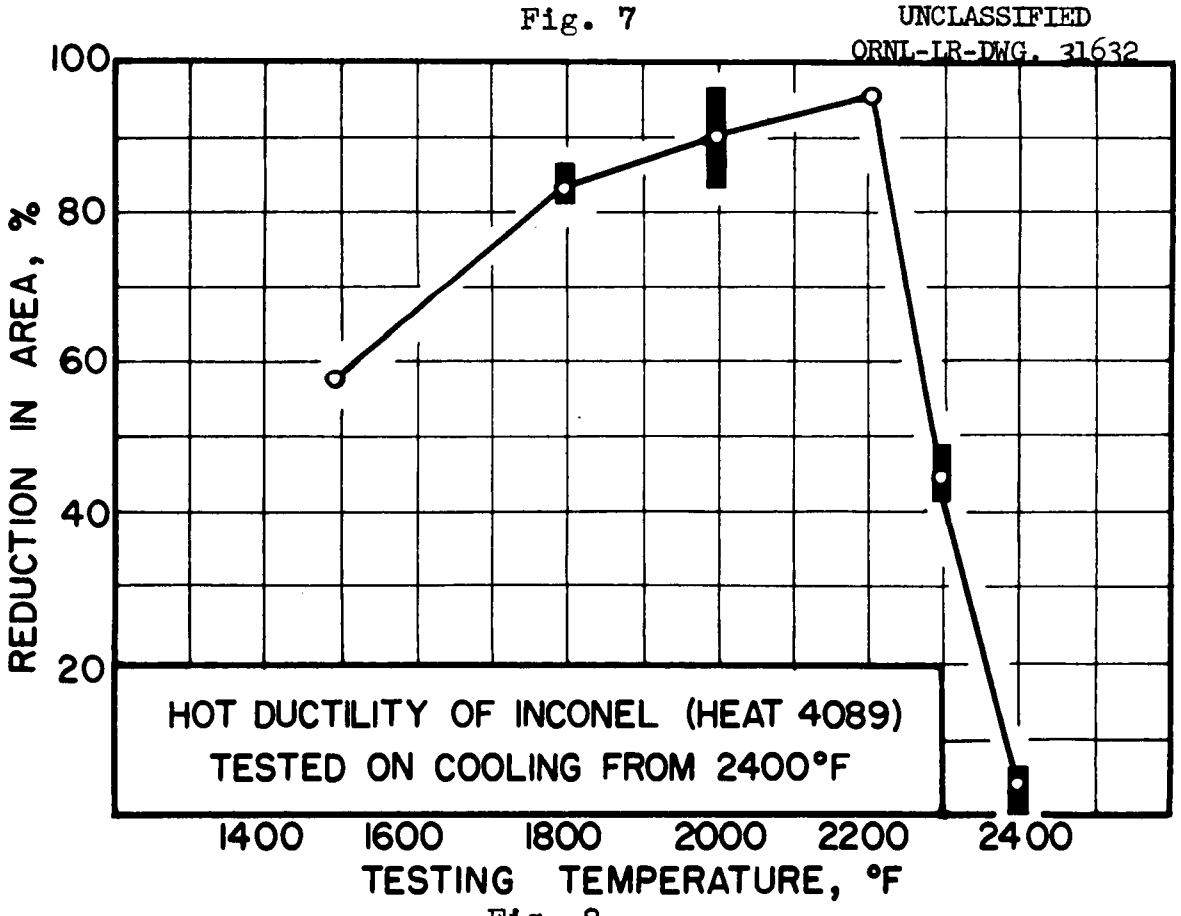
UNCLASSIFIED
ORNL-LR-DWG. 31632
100
80
60
40
20
REDUCTION IN AREA, %
HOT DUCTILITY OF INCONEL (HEAT 4089)
TESTED ON COOLING FROM 2400°F
1400
1600
1800
2000
2200
2400
TESTING TEMPERATURE, °F

Fig. 8

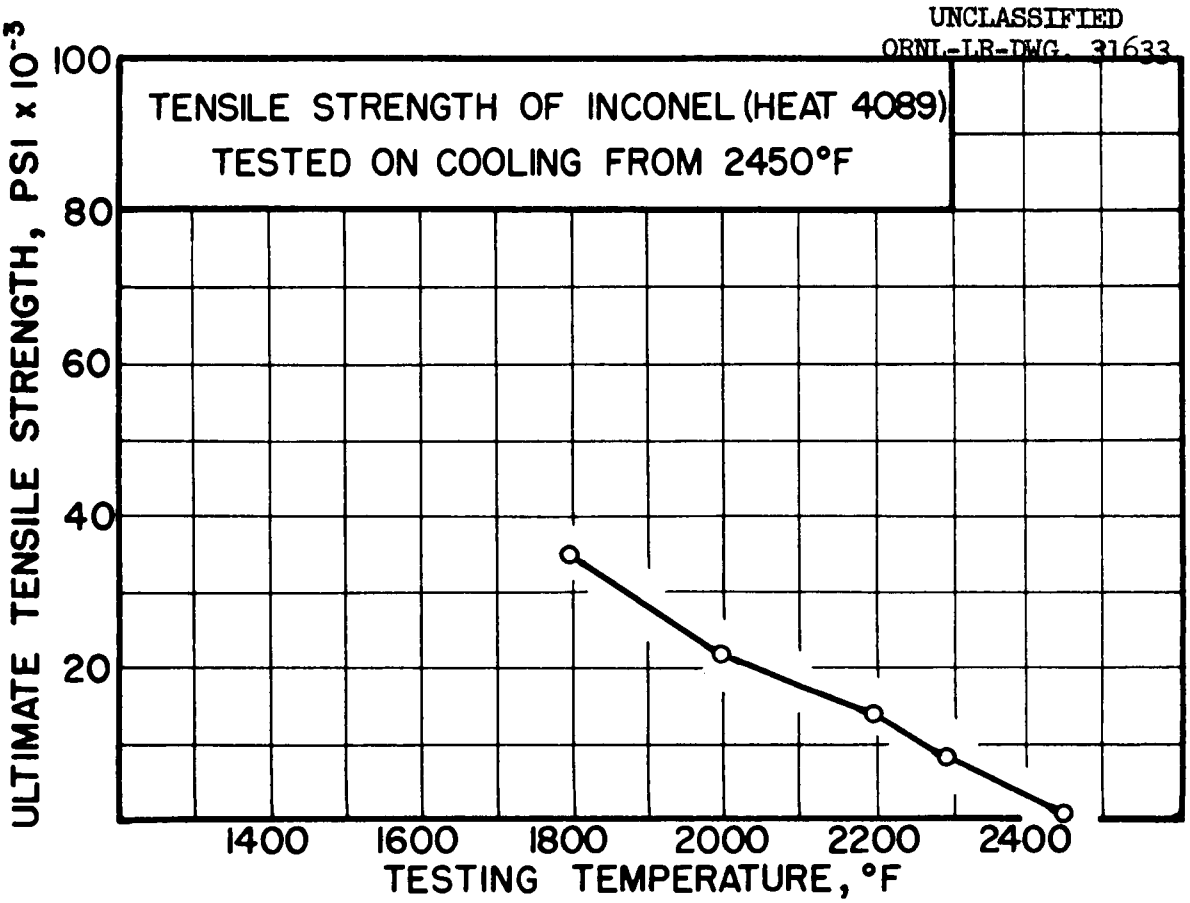
UNCLASSIFIED
ORNL-LR-DWG. 31633
TENSILE STRENGTH OF INCONEL (HEAT 4089)
TESTED ON COOLING FROM 2450°F
ULTIMATE TENSILE STRENGTH, PSI x 10⁻³
100
80
60
40
20
1400
1600
1800
2000
2200
2400
TESTING TEMPERATURE, °F

Fig. 9

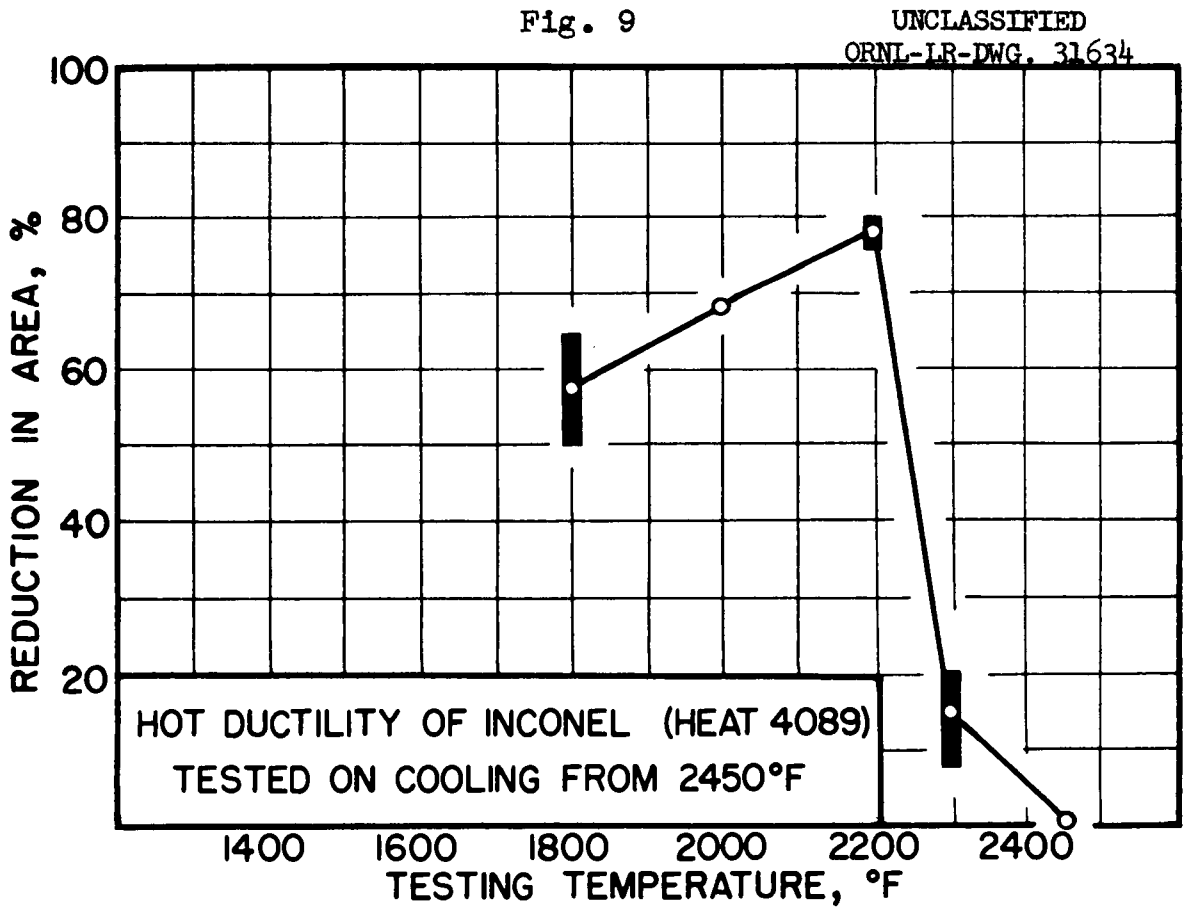
UNCLASSIFIED
ORNL-LR-DWG. 31634
REDUCTION IN AREA, %
100
80
60
40
20
HOT DUCTILITY OF INCONEL (HEAT 4089)
TESTED ON COOLING FROM 2450°F
1400
1600
1800
2000
2200
2400
TESTING TEMPERATURE, °F

Fig. 10

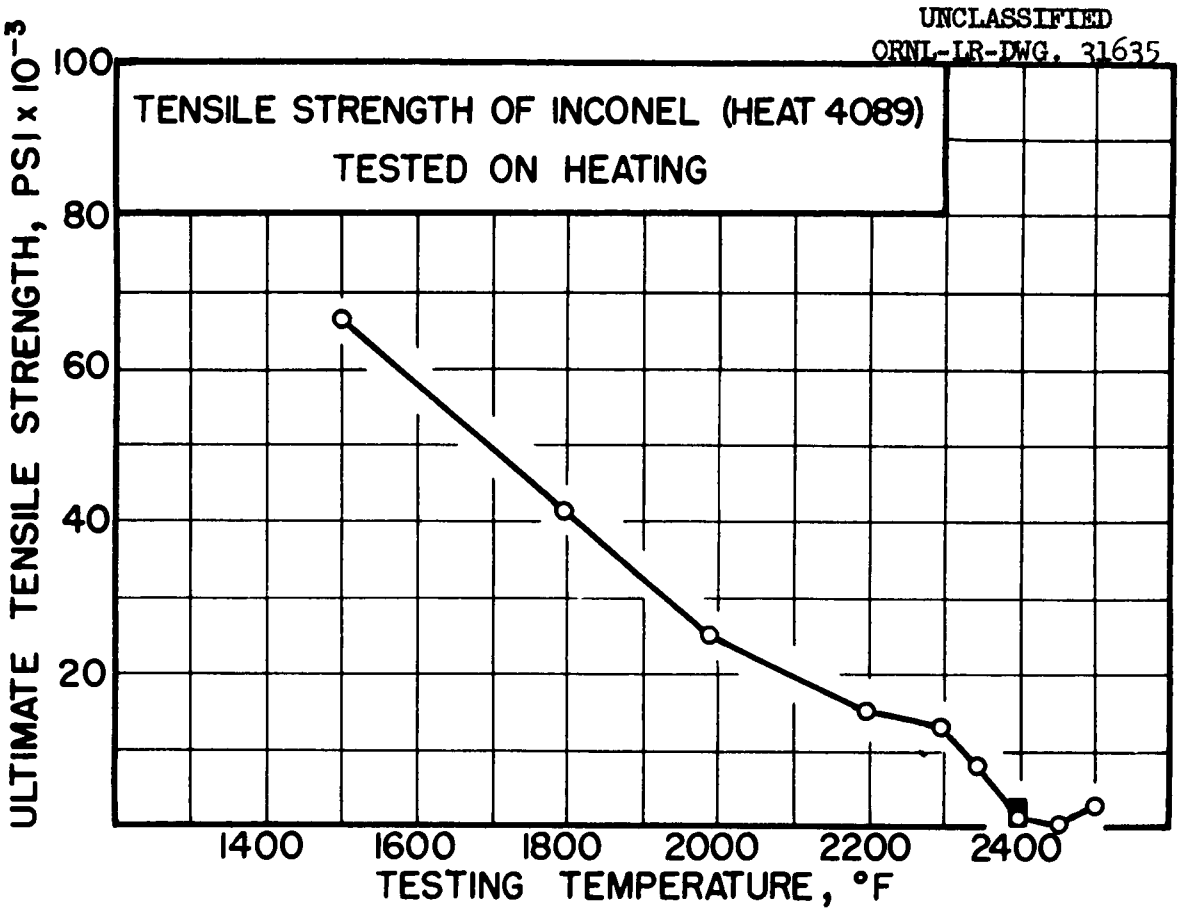
UNCLASSIFIED
ORNL-LR-DWG. 31635
TENSILE STRENGTH OF INCONEL (HEAT 4089)
TESTED ON HEATING
ULTIMATE TENSILE STRENGTH, PSI x 10⁻³
100
80
60
40
20
1400
1600
1800
2000
2200
2400
TESTING TEMPERATURE, °F

Fig. 11

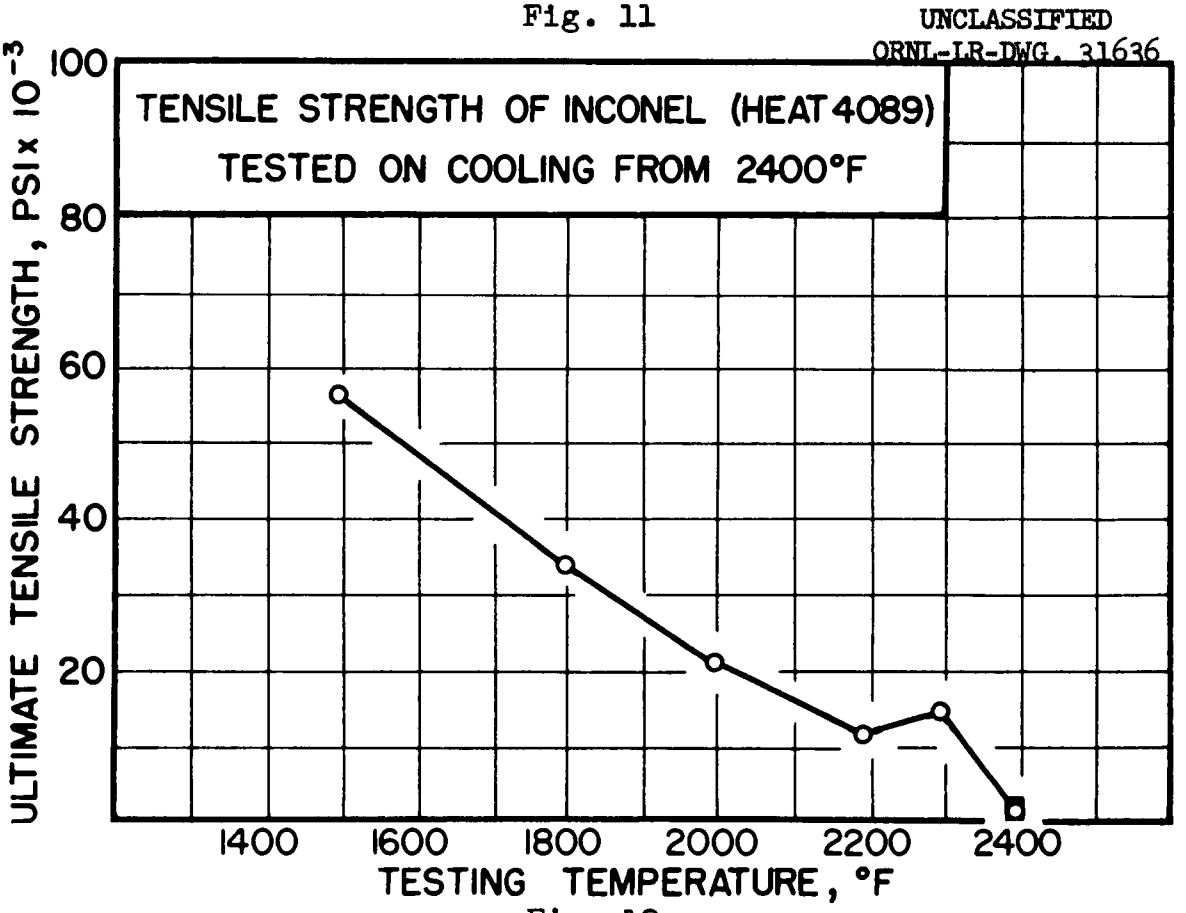
UNCLASSIFIED
ORNL-LR-DWG. 31636
TENSILE STRENGTH OF INCONEL (HEAT 4089)
TESTED ON COOLING FROM 2400°F
ULTIMATE TENSILE STRENGTH, PSI x 10⁻³
100
80
60
40
20
1400
1600
1800
2000
2200
2400
TESTING TEMPERATURE, °F

Fig. 12

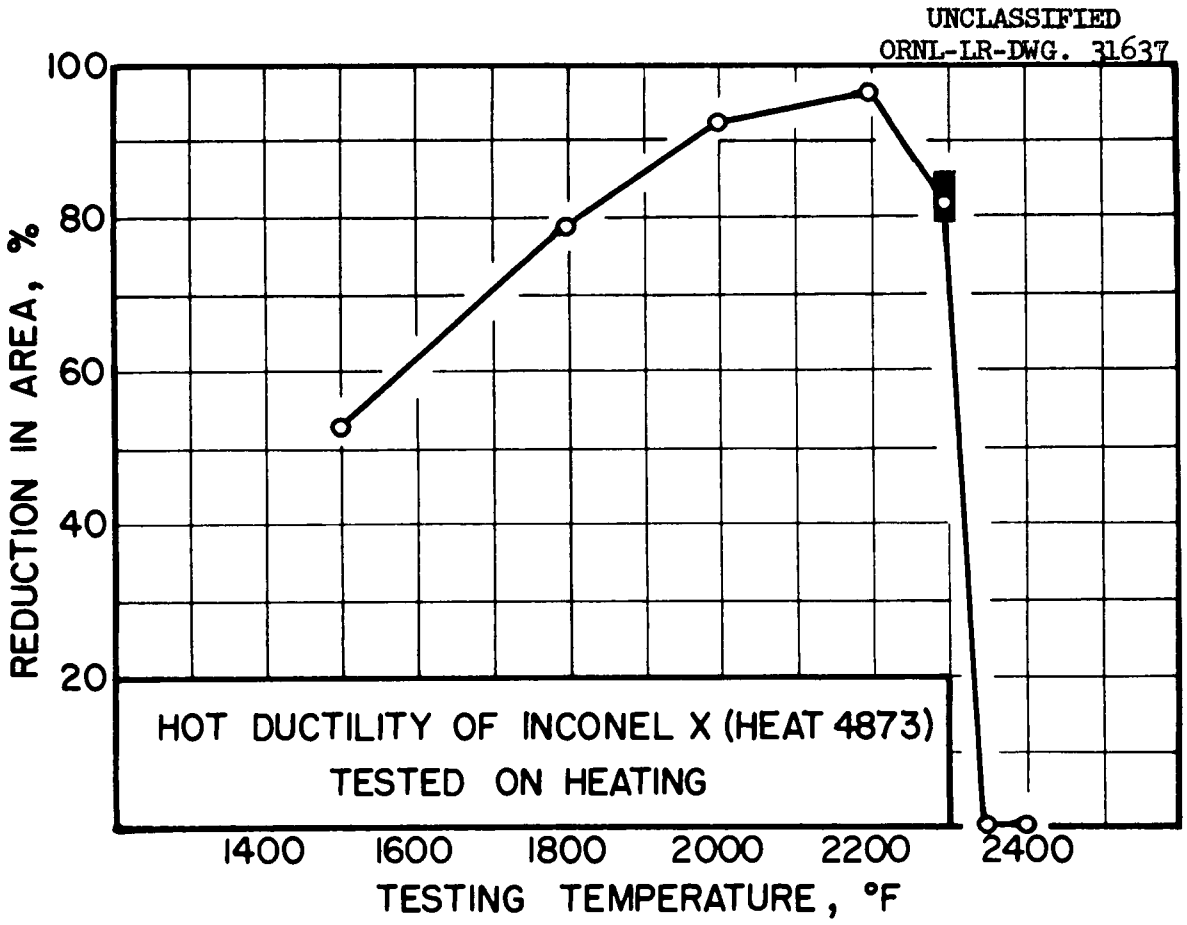
UNCLASSIFIED
ORNL-LR-DWG. 31637
100
80
60
40
20
REDUCTION IN AREA, %
HOT DUCTILITY OF INCONEL X (HEAT 4873)
TESTED ON HEATING
1400
1600
1800
2000
2200
2400
TESTING TEMPERATURE, °F

Fig. 13

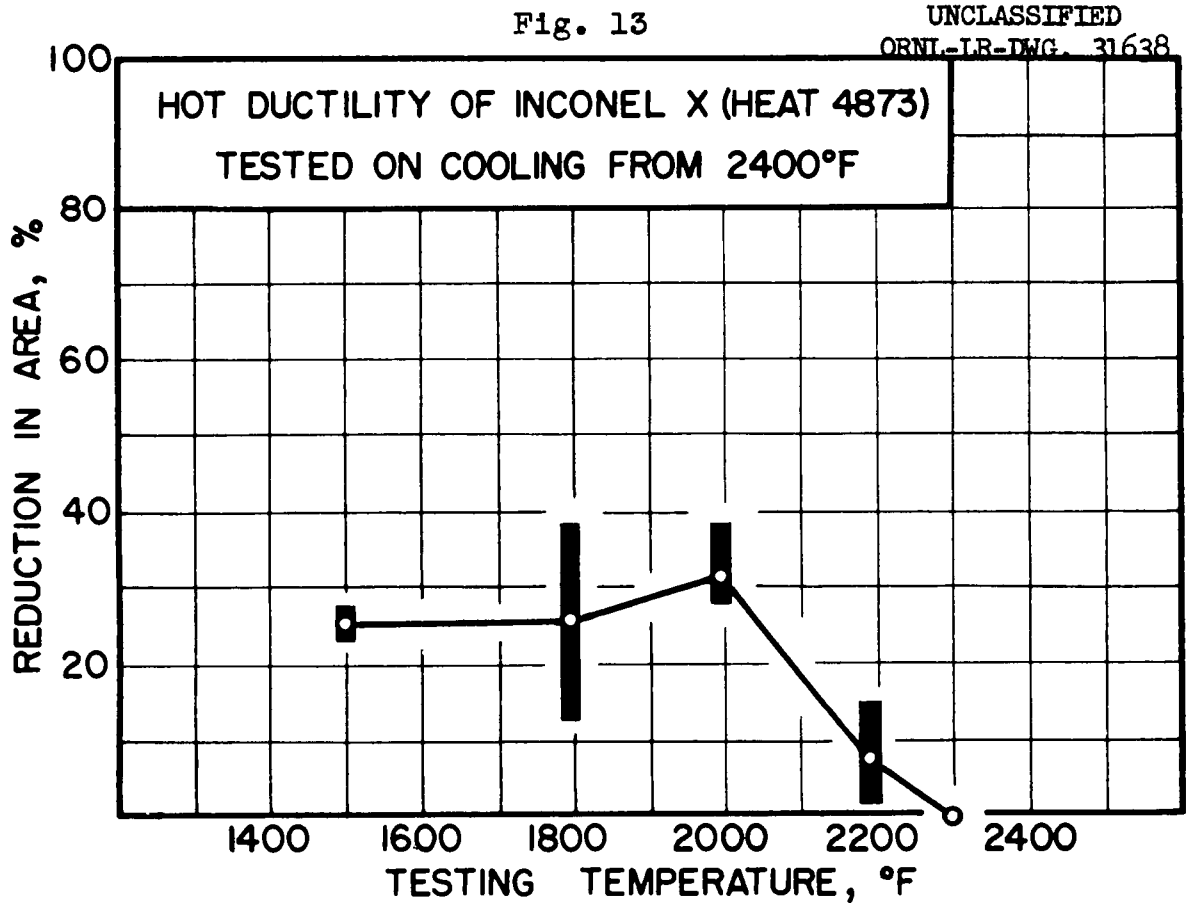
UNCLASSIFIED
ORNL-LR-DWG. 31638
100
80
60
40
20
REDUCTION IN AREA, %
HOT DUCTILITY OF INCONEL X (HEAT 4873)
TESTED ON COOLING FROM 2400°F
1400
1600
1800
2000
2200
2400
TESTING TEMPERATURE, °F

Fig. 14

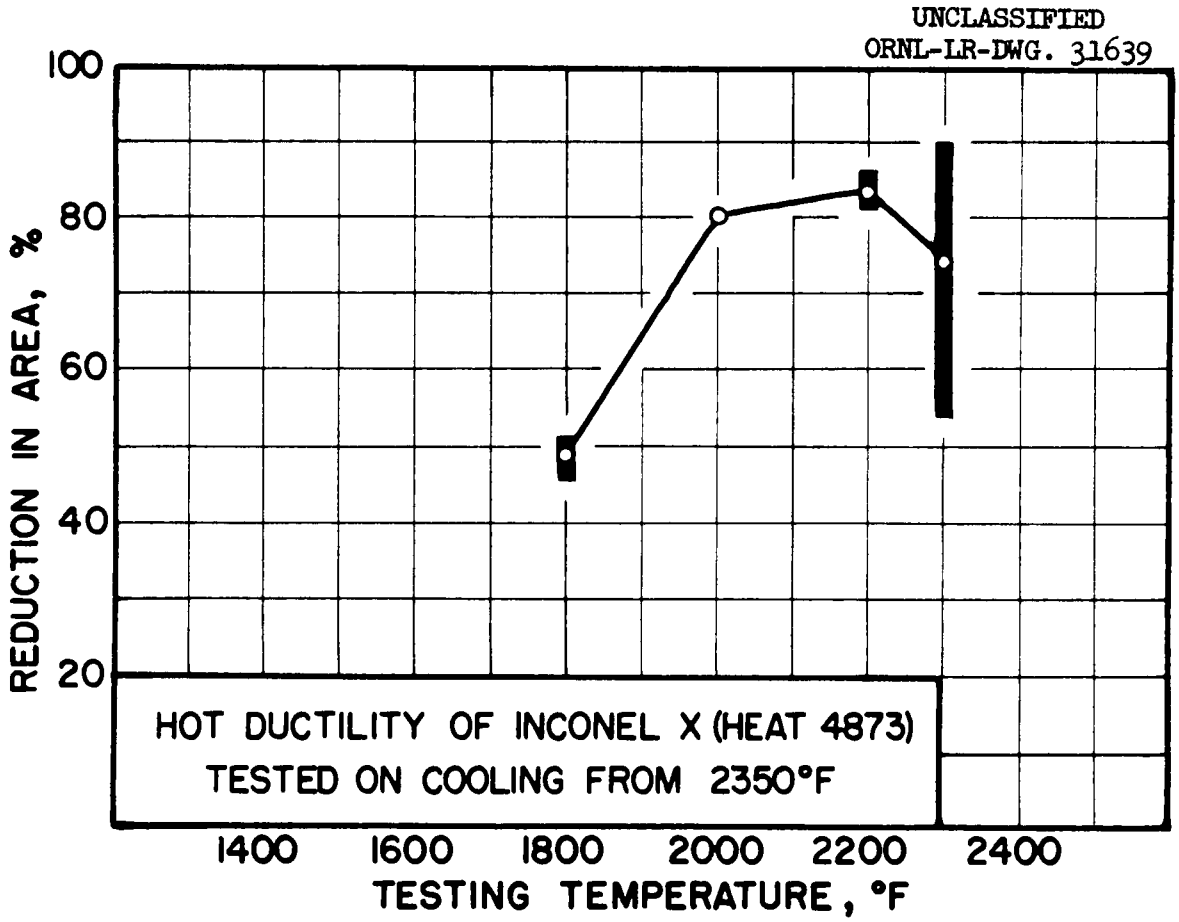
UNCLASSIFIED
ORNL-LR-DWG. 31639
REDUCTION IN AREA, %
100
80
60
40
20
HOT DUCTILITY OF INCONEL X (HEAT 4873)
TESTED ON COOLING FROM 2350°F
1400
1600
1800
2000
2200
2400
TESTING TEMPERATURE, °F

Fig. 15

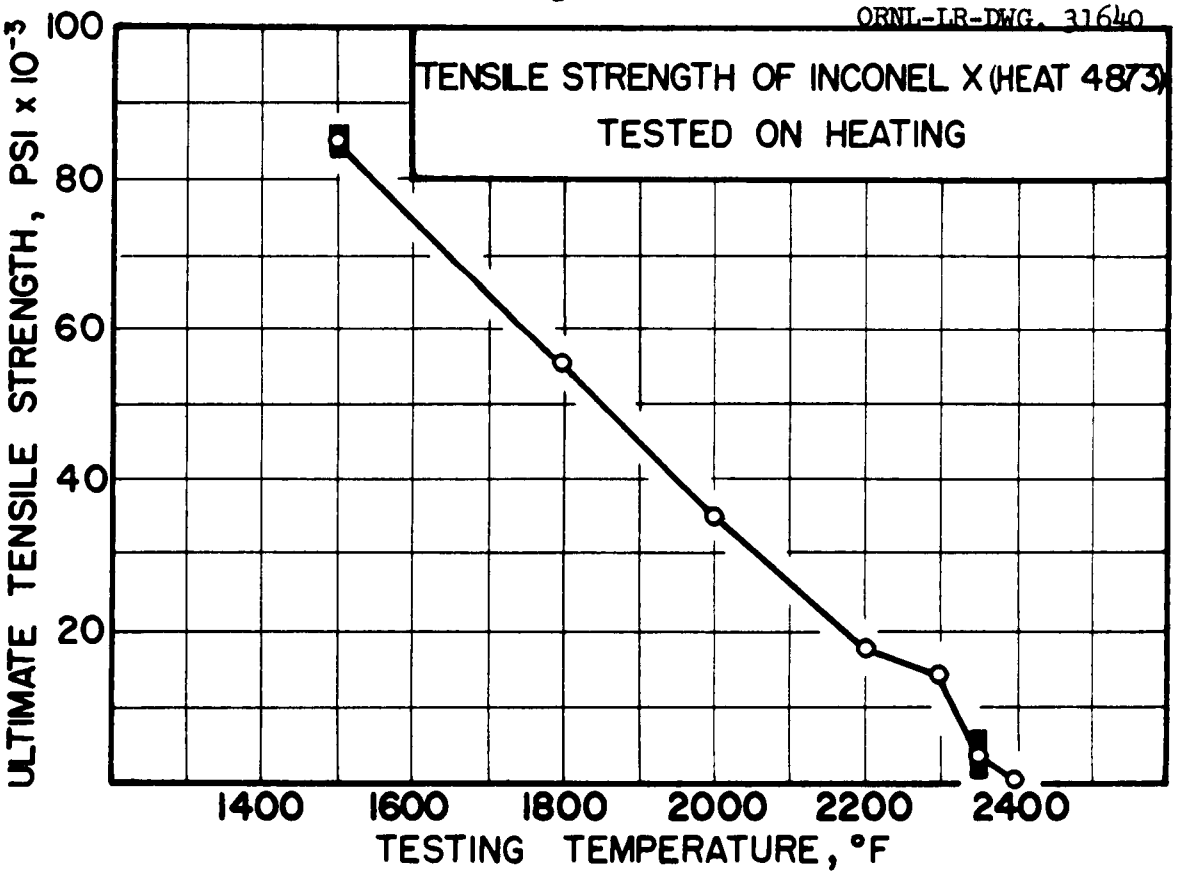
UNCLASSIFIED
ORNL-LR-DWG. 31640
ULTIMATE TENSILE STRENGTH, PSI x 10⁻³
100
80
60
40
20
TENSILE STRENGTH OF INCONEL X (HEAT 4873)
TESTED ON HEATING
1400
1600
1800
2000
2200
2400
TESTING TEMPERATURE, °F

Fig. 16

point attain the lowest value of the on-heating curve. Along with this drastic loss in ductility, the tensile strength is reduced markedly at all testing temperatures as is evident by comparing Fig. 16 and 17.

Tables XI and XII tabulate the results of specimens heated to 2400°F for Inconel and 2350°F for Inconel X in both cases, 50°F below the damaging temperature and fractured along the cooling portion of the thermal cycle.

Figures 8 and 12 summarize these on-cooling data in Table XI for Inconel. In Fig. 8 the hot ductility curve is shown to have the characteristic increase in ductility up to a peak value of 2200°F and a sharp decrease to 2400°F. While the curve in general never quite reaches the on-heating curve ductility values, Fig. 7, the only marked decrease in ductility occurs at the 2300°F value. The ultimate tensile strength values, as may be seen by comparing Figs. 1 and 12 are slightly affected by this thermal treatment cycle at the higher temperatures, with a small reduction of the tensile strength at the lower test temperatures.

A plot of the per cent reduction in area for Inconel X heated to 50° below the damaging temperature is shown in Fig. 15. Hot ductility is observed to vary in a characteristic manner rising to 2200°F and dropping at more elevated temperatures. Damage is not as severe as at the temperature of 2400°F, Fig. 14, but at all temperatures the ductility is lowered from the on-heating values, Fig. 13. The ultimate tensile strength as summarized in Fig. 18 for the conditions in Table XII, can be seen by comparison to Fig. 16, to have suffered some reduction at the lower temperatures but compares favorably at the higher test temperature.

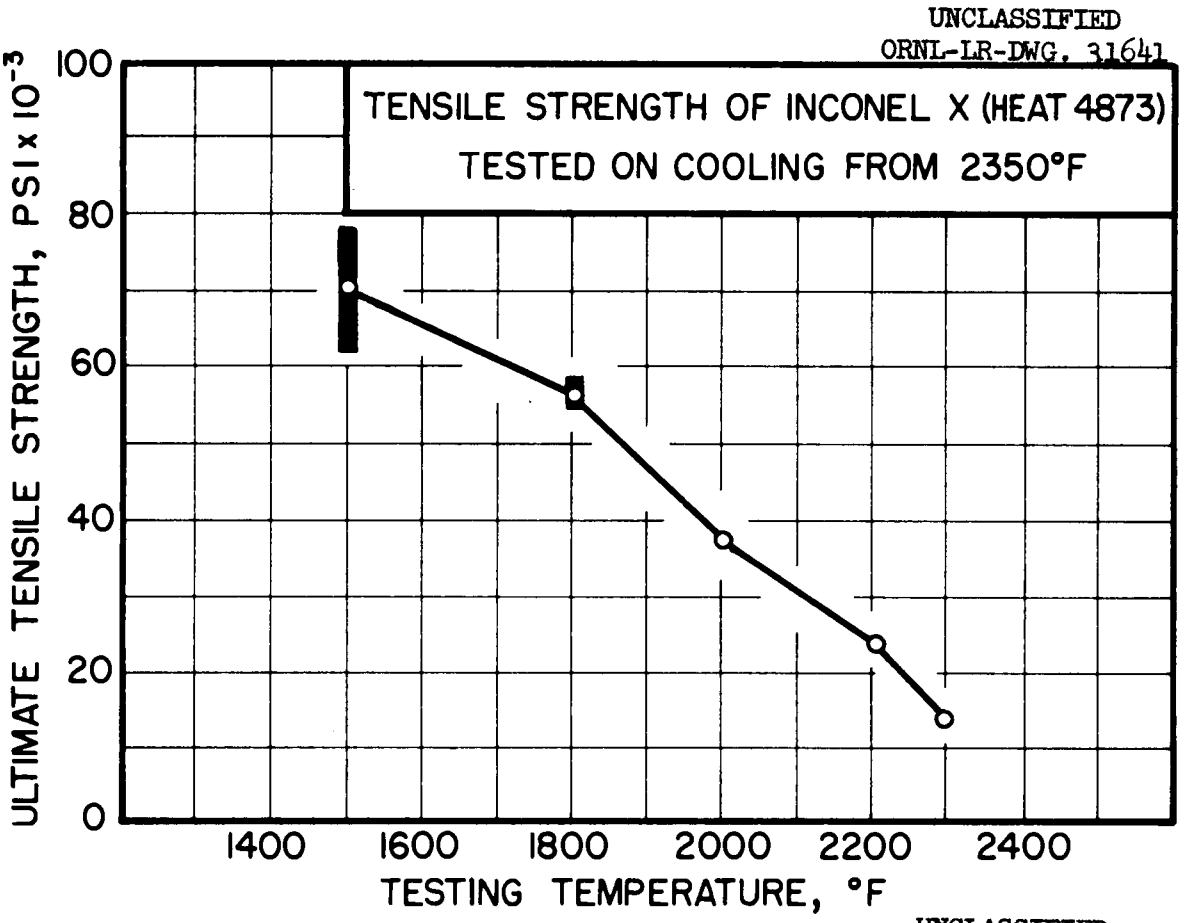
UNCLASSIFIED
ORNL-LR-DWG. 31641
TENSILE STRENGTH OF INCONEL X (HEAT 4873)
TESTED ON COOLING FROM 2350°F
ULTIMATE TENSILE STRENGTH, PSI x 10⁻³
100
80
60
40
20
0
1400
1600
1800
2000
2200
2400
TESTING TEMPERATURE, °F

Fig. 17

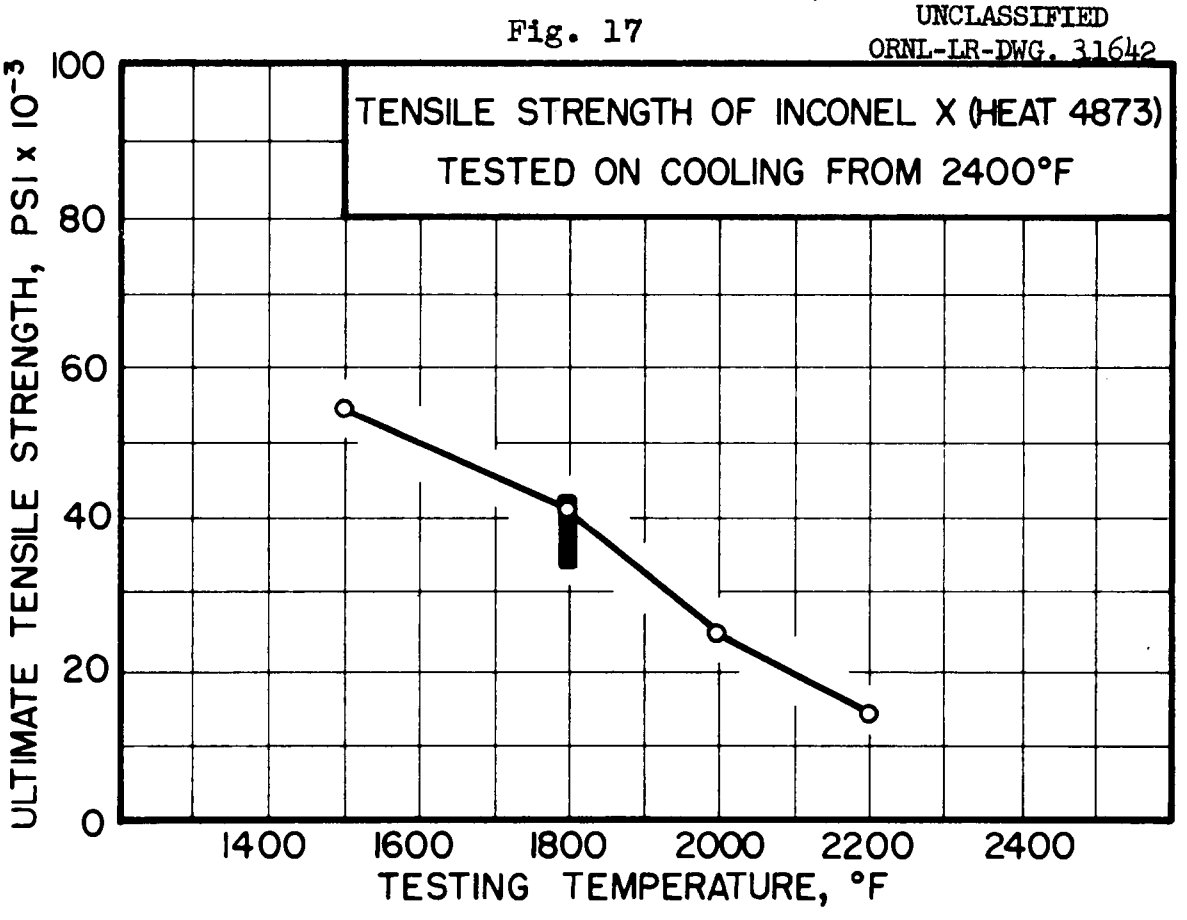
UNCLASSIFIED
ORNL-LR-DWG. 31642
TENSILE STRENGTH OF INCONEL X (HEAT 4873)
TESTED ON COOLING FROM 2400°F
ULTIMATE TENSILE STRENGTH, PSI x 10⁻³
100
80
60
40
20
0
1400
1600
1800
2000
2200
2400
TESTING TEMPERATURE, °F

Fig. 18

METALLOGRAPHIC INVESTIGATION

From each test temperature a metallographic specimen was selected, which had a reduction in area value closest to the mean value for that temperature. The specimen was sectioned, mounted longitudinally, etched electrolytically with 5% sulfuric acid, and examined under various magnifications. The photomicrographs included are of fractured specimens taken at 100X or 1000X and are arranged in series of three. In Fig. 19a, 19b, and 19c we have consecutively, specimens of Inconel fractured at 2000°F, 2200°F and 2300°F while cooling from 2400°F, at 100X. The 2000°F sample has the smallest grain size and shows a deformation texture where the specimen elongated before fracture. The deformation texture does not stand out as much in the 2200°F sample but can be observed. The grain size is not as fine or uniform as in the 2000°F specimen. In Fig. 19a, 19b, and 19c the main difference is in the larger grain size and in the more brittle fracture for the 2300°F specimens. At higher magnifications an examination of the grain boundaries does not reveal any significant difference between the specimens. These are included in Fig. 20a, 20b, and 20c. All three exhibit the same type of sharp, uneven grain boundaries.

Specimens of Inconel X fractured on cooling from 2400°F are shown in Fig. 21a, 21b, and 21c at 2000°F, 2200°F, and 2300°F at 100X. The 2000°F specimen shows the intergranular fracture with incomplete recrystallization due to deformation at this temperature. The 2200°F fracture very clearly indicates the intergranular nature of the fracture as does the 2300°F specimen. These are the severely damaged specimens which lost almost all ductility upon heating to 2400°F. Fig. 22a, 22b, and 22c are photomicrographs of the same specimens taken at 1000X. This intergranular fracture is seen in the 2300°F specimen, and grain boundary melting is observed in Fig. 22a and 22b. In both, the edges of the grains are rounded, and melting is especially noticed in the triple points where the grains meet.

Fractured specimens of Inconel X heated to 2350°F or 50° below the damaging temperature are shown at 100X in Fig. 23a, 23b, and 23c. The 2300°F specimen exhibits a finer grain size than Inconel X heated to the damaging temperature and shows some deformation texture. The 2200°F fracture has a finer structure with an intergranular fracture. Recrystallization is much more complete in the 2000°F specimen but still shows areas of elongated grains deformed in the direction of fracture.

UNCLASSIFIED
PHOTO 44536

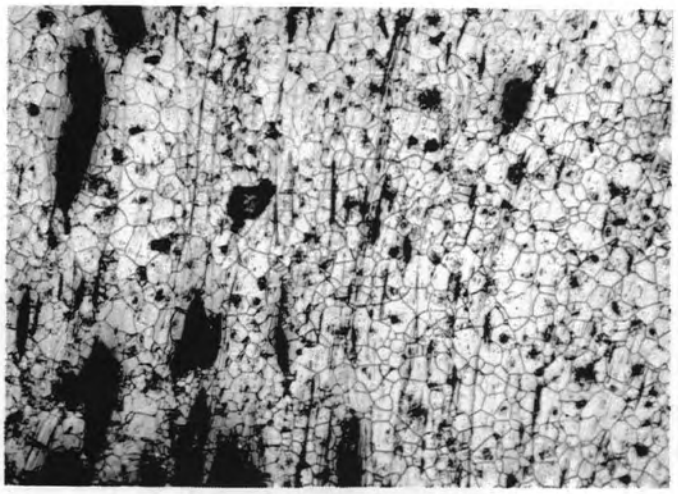

(a) Inconel heated to 2400°F and fractured at 2000°F
100X

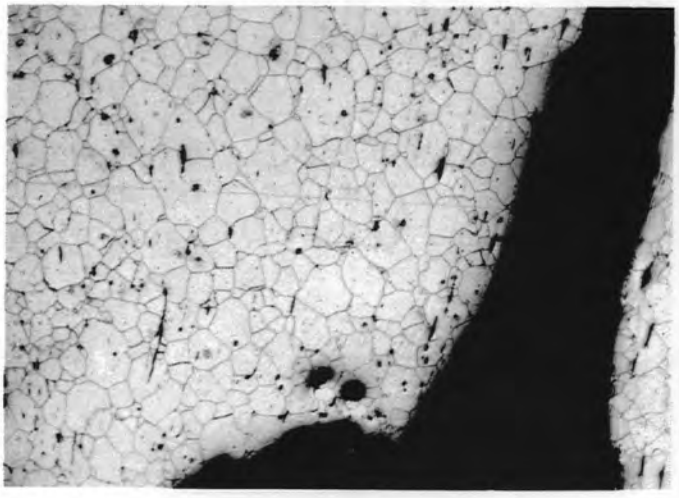

(b) Inconel heated to 2400°F and fractured at 2200°F
100X

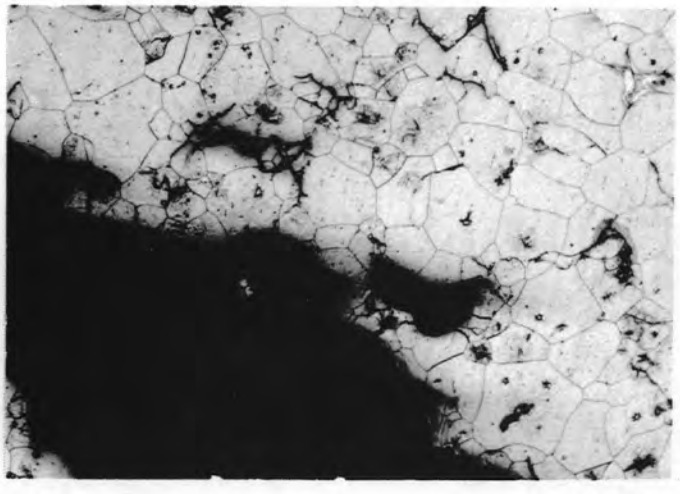

(c) Inconel heated to 2400°F and fractured at 2300°F
100X

Fig. 19

UNCLASSIFIED
PHOTO 44537

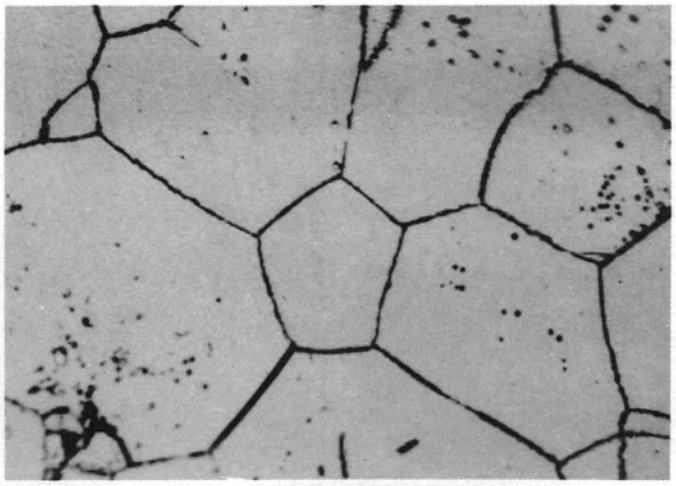

(a) Inconel heated to 2400°F and fractured at 2000°F
1000X

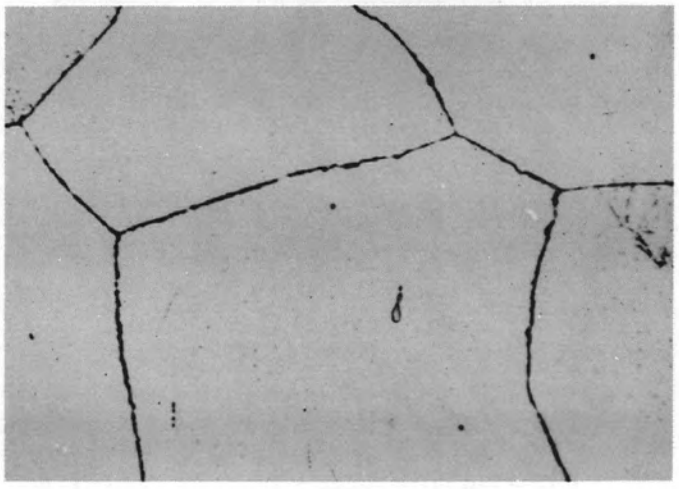

(b) Inconel heated to 2400°F and fractured at 2200°F
1000X

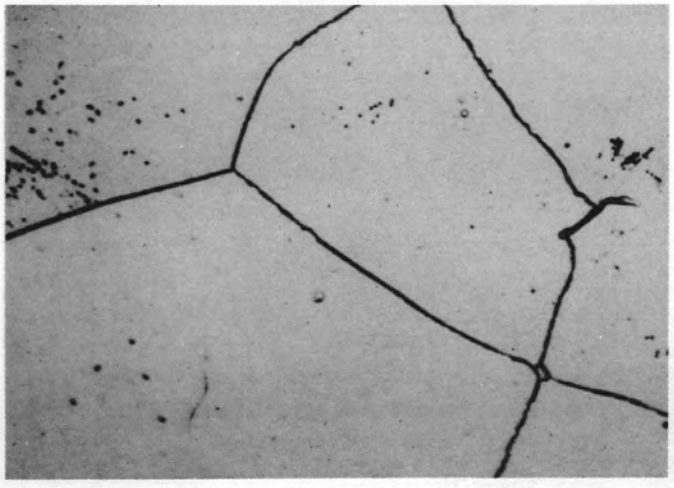

(c) Inconel heated to 2400°F and fractured at 2300°F
1000X

Fig. 20

UNCLASSIFIED
PHOTO 44538

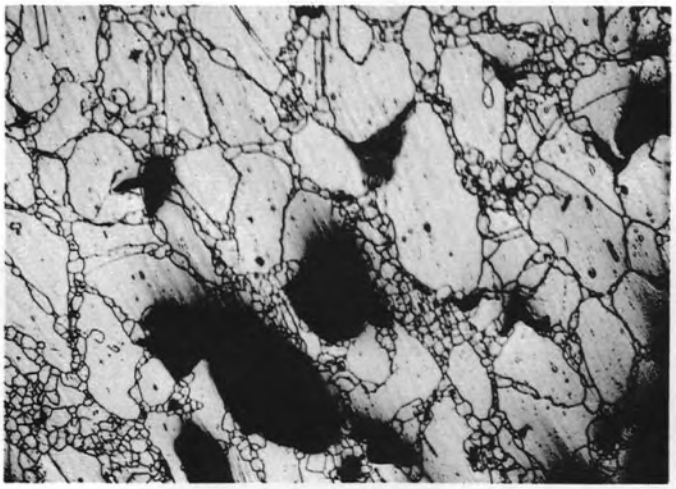

(a) Inconel X heated to 2400°F and fractured at 2000°F
100X

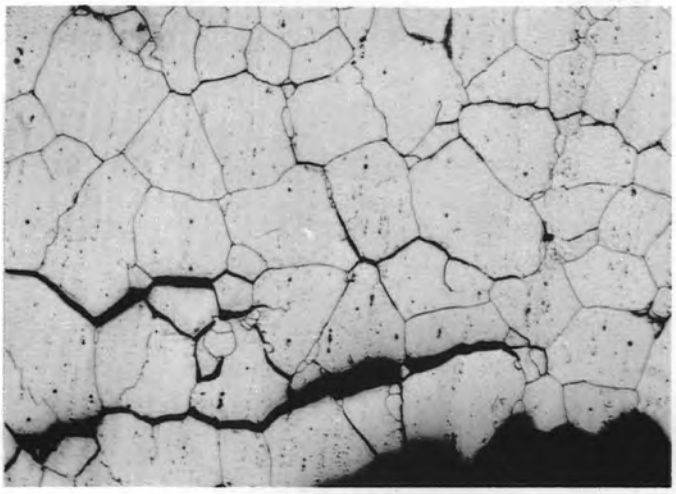

(b) Inconel X heated to 2400°F and fractured at 2200°F
100X

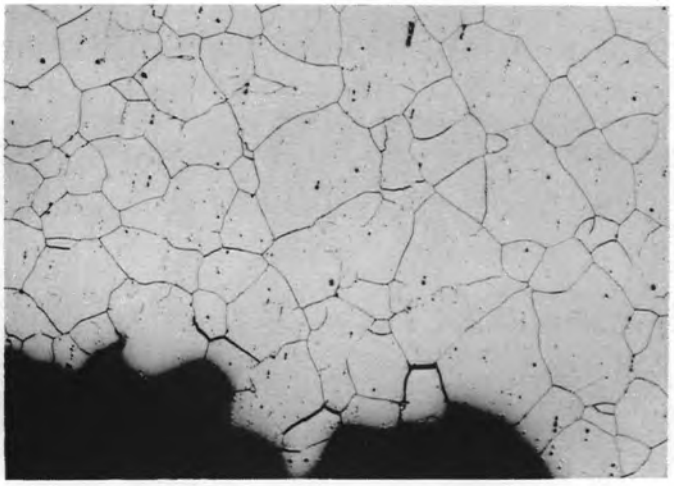

(c) Inconel X heated to 2400°F and fractured at 2300°F
100X

Fig. 21

UNCLASSIFIED
PHOTO 44539

(a) Inconel X heated to 2400°F and fractured at 2000°F
1000X

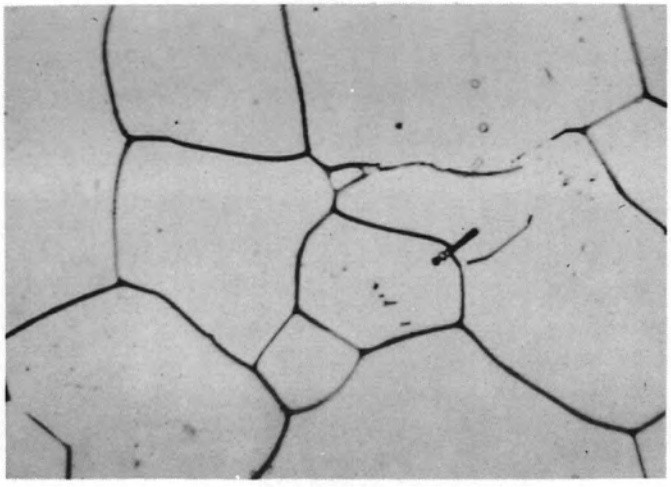

(b) Inconel X heated to 2400°F and fractured at 2200°F
1000X

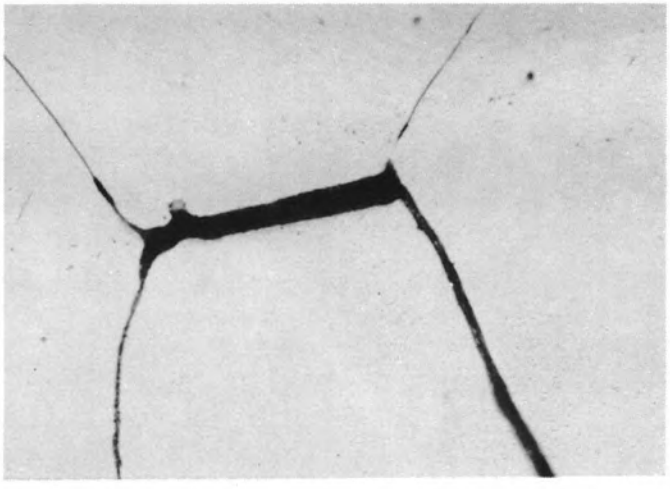

(c) Inconel X heated to 2400°F and fractured at 2300°F
1000X

Fig. 22

UNCLASSIFIED
PHOTO 44540

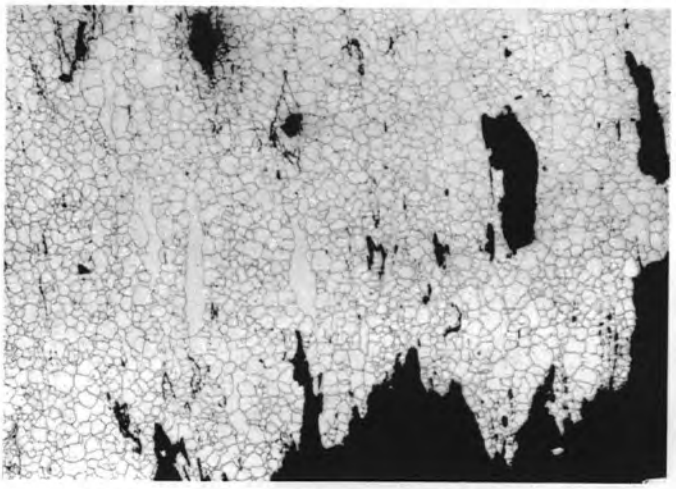

(a) Inconel X heated to 2350°F and fractured at 2000°F
100X

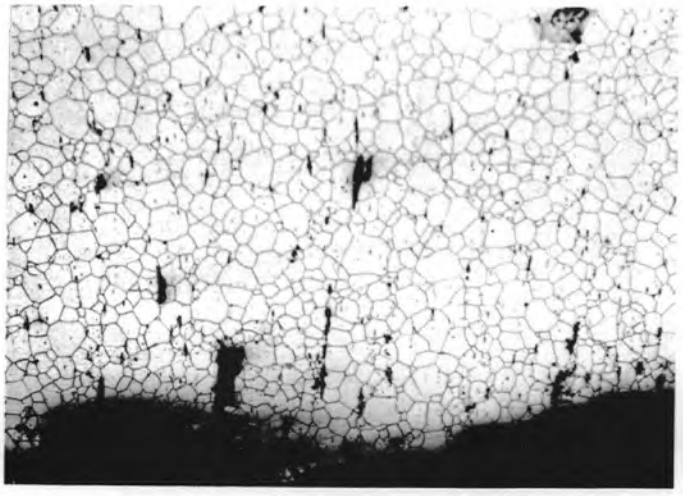

(b) Inconel X heated to 2350°F and fractured at 2200°F
100X

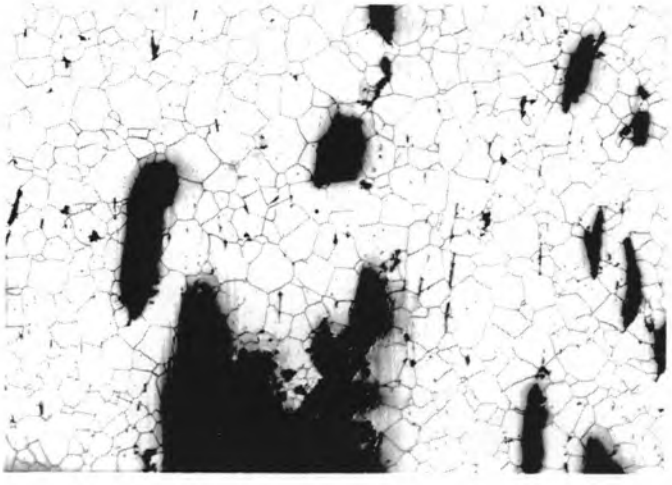

(c) Inconel X heated to 2350°F and fractured at 2300°F
100X

Fig. 23

An examination of the same structures at 1000X are shown in Fig. 24a, 24b, and 24c. In all of the specimens, grain boundary melting can be seen at the triple points of the grain boundaries. The extent of melting is limited to these triple points and is not in the form of intergranular rivers[7] as in Fig. 22a, damaged by the higher temperature thermal cycle.

The Inconel specimens fractured on cooling from 2450°F thermal cycle also showed some evidences of grain boundary melting. The grain boundary melting in Inconel, however, is scattered between isolated grams and not as continuous as the melting of Inconel X, Fig. 22, fractured on cooling from 2400°F.

UNCLASSIFIED
PHOTO 44541

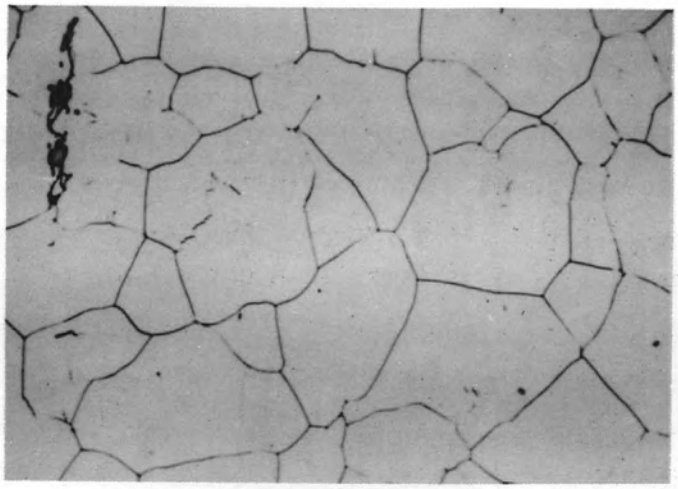

(a) Inconel X heated to 2350°F fractured at 2000°F
1000X

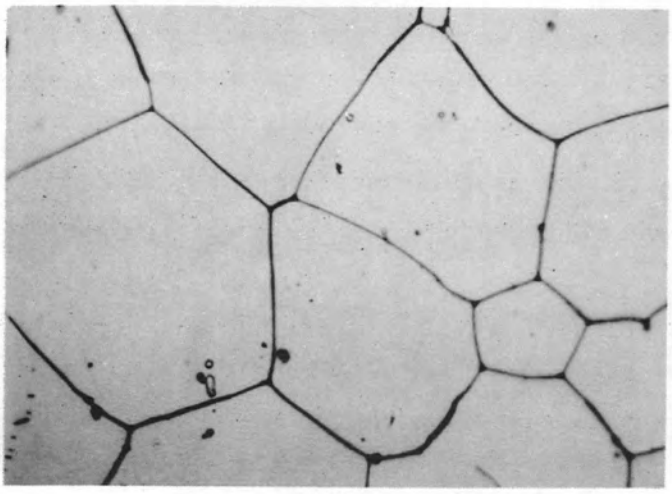

(b) Inconel X heated to 2350°F and fractured at 2200°F
1000X

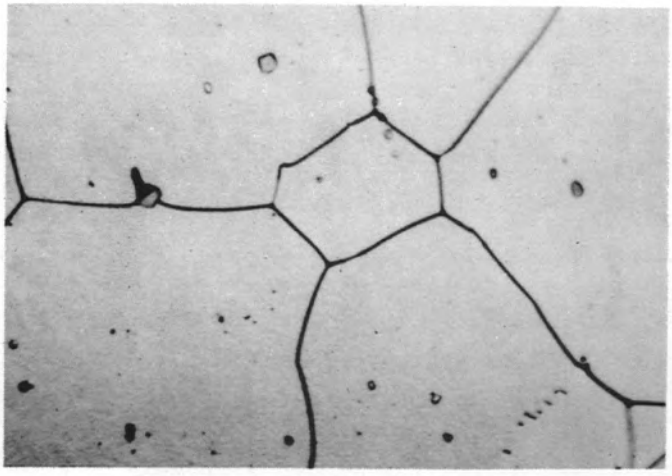

(c) Inconel X heated to 2350°F and fractured at 2300°F
1000X

Fig. 24

DISCUSSION

The result of the per cent reduction in area increasing with temperature is not surprising since at higher temperatures the yield strength decreases and plastic deformation requires less force. This is in agreement with the lowering of the ultimate tensile strength as a function of the testing temperature in all the thermal cycles investigated for both of the materials tested.

The transition from ductile to brittle fracture at test temperatures above 2200°F bears out known plastic properties of metals. According to Seitz,[8] grain boundaries are transition layers of atoms thermodynamically less stable than the interior atoms. At temperatures not too near the melting point, grain boundaries exhibit good strengths, and fractures occur most commonly through grains rather than at their boundaries in rupture tests performed well below the melting temperature. For higher temperatures near the melting point of the bulk material, the relative instability of the grain boundaries increases and cracks follow such boundaries. All fractures observed in this investigation followed this same general pattern.

A comparison of Figs. 7, 8, and 10 for Inconel fractured on heating, on cooling from 2400°F, and on cooling from 2450°F, respectively, indicates that the material is slightly damaged by the 2400°F thermal cycle and damage incurred by the 2450°F thermal cycle is still not too severe.

The severe damage to the ductility of Inconel X exposed to the 2400°F thermal cycle is shown in Fig. 14 when compared to the on-heating and on-cooling from 2350°F values in Figs. 13 and 15. The percentage loss in ductility is 100% at 2300°F, 92.0% at 2200°F and 65.5% at 2000°F compared to 82.5% at 2300°F, 20.9% at 2200°F and 30.6% at 2000°F for Inconel from the damaging thermal cycle of 2450°F. The drastic loss in ductility for Inconel X corroborates the sponsor 's difficulties in welding Inconel X in heavy sections whereas Inconel, which exhibited a smaller loss in ductility, was satisfactorily welded.

The photomicrographs of specimens of Inconel X fractured on-cooling from 2400°F in Fig. 22a and 22b clearly show evidence of grain boundary melting by the rounding of the grains and smoothness of the boundaries. Further substantiation of the grain boundary melting is observed in the triple points of the grains of specimens of Inconel X fractured on-cooling from 2350°F shown in Fig. 24a, 24b, and 24c.

Inconel X exhibits a more continuous type of grain boundary melting than does Inconel for specimens fractured from their respective embrittling temperatures. Correlation between the drastic loss in ductility and the incidence of grain-boundary melting indicates that the melting in the grain boundaries is in some way tied in with the mechanism for the severe embrittlement of Inconel X during the 2400°F thermal cycle.

A solid-liquid transition expansion in the grain boundaries will impose a stress on the matrix which at the high temperatures has a low yield strength. Upon cooling, the melted material will shrink with resolidification. Shrinkage could be accompanied with the formation of fine micro-cracks in areas where strain was produced in the matrix by the solid liquid expansion creating larger areas for the grain boundary material to fill.

It is possible that the severe damage to Inconel X occurs in some such manner. Inconel, on the other hand, exhibits a limited amount of grain boundary melting which would not be expected to severely damage the material.

SUMMARY AND CONCLUSIONS

Modifications to the existing hot-ductility apparatus enables the measurement and recording of the load necessary to fracture a specimen at any desired point in a thermal cycle.

The hot ductility and ultimate tensile strength of Inconel and Inconel X were investigated under three conditions using thermal cycles experienced in an arc weld on 1 1/2-in. plate with 70,000 joules input.

1. Specimens were fractured on-heating to a peak value until a temperature was reached where the ductility was reduced to zero. This temperature was considered the embrittling temperature.
2. Specimens were fractured on-cooling from the embrittling temperature, which was 2450°F for Inconel and 2400°F for Inconel X.
3. Specimens were fractured on-cooling from 50° below the embrittling temperature. For Inconel, this temperature was 2400°F and for Inconel X, 2350°F.

The hot ductility of both alloys tested for the first condition was found to increase with the testing temperature until a peak value was attained at 2200°F. At temperatures from 2200°F to the embrittling temperature the ductility decreased rapidly; over the testing range from 1500°F to the embrittling temperature the ultimate tensile decreased with temperature.

A severe loss in ductility is noted for Inconel X tested under the second condition when compared to the on-heating condition. A marked reduction in tensile strength is also noted for all temperatures. A comparison of Inconel for the second condition with the on-heating results reveals a general lowering of ductility, but still retains the general characteristic shape of an increase to 2200°F, followed by a sharp decrease to 2450°F. The tensile strength is lowered at the lower test temperatures but exhibits almost no difference at the higher temperatures from the on-heating values.

Metallographic examination of the fractured specimens revealed that the drastic loss in ductility is accompanied with grain-boundary melting in Inconel X.

Correlation between the poor weldability of Inconel X in thick sections with the severe loss in ductility and the satisfactory weldability of Inconel with a slight loss in ductility would indicate that this method of testing could predict the weldability of other alloys.

REFERENCES

1. "Engineering Properties of Inconel and Inconel X." Tech. Bull. T-7, International Nickel Co., Inc.

2. Cross, H. C., and Fruman, J. W. "Office of Naval Research and NACA Metallurgical Investigation of a Forged Disc of Inconel X Alloy."

3. Apblett, W. R., and Pellini, W. S. "Factors Which Influence Weld Hot Cracking." The Welding Journal, 34 (2), Research Suppl., 83-S to 90-S, (1954).

4. Nippes, E. F., and Savage, W. F. "Development of Specimens Simulating Weld Heat-Affected Zones." The Welding Journal, 28, 534s-546s, (1949).

5. Nippes, E. F. et al. "An Investigation of the Hot Ductility of High-Temperature Alloys." The Welding Journal, 34, 183s-196s, (1955).

6. Nippes, E. F., et al. "Some Properties of the Heat-Affected Zone in Arc Welded Type 347 Stainless Steel." The Welding Journal, 34 (-4), Research Suppl., 169s-196s, (April, 1955).

7. Nippes, E. F., and Fishman, H. B. "Optimum Spot and Seam Welding Conditions for Inconel X." The Welding Journal, 34 (1), Research Suppl. 1-s to 14-s, (1954).

8. Seitz, F. The Physics of Metals. New York: McGraw-Hill, (1943).

APPENDIX

CALIBRATION

Before actual experimental work could be done, calibration of the two load cells and the effect of varying voltage of the source on the load cell had to be considered. The load cells were calibrated by mounting them in a Southwerk-Emery tensile machine and applying loads up to the maximum for each cell. In order to find how reduced voltage would affect the calibration curve, a calibration was run under reduced voltage.

For daily calibration, a series of resistors were connected to give a shunt calibration curve without going to a tensile machine. The shunt method consisted of unbalancing one arm of the bridge by connecting a resistance in parallel with the arm. The unbalance corresponded to a definite amount of load, so that while the curve may shift due to reduced voltage, a new calibration curve can be gotten in the matter of minutes. It was found that curves did not vary much from day to day except when batteries were left on for prolonged periods of time.

The temperature galvanometer was also calibrated each day to insure accurate data. A known source of millivoltage was introduced over the range of temperature at which the specimens were fractured and the galvanometer deflection was determined as a function of temperature. The strain transducer was calibrated by using a micrometer depth gauge comparing actual displacement to galvanometer deflection.

PRELIMINARY PROCEDURE

When the stock was received, it was coded as to letter series and color of paint to distinguish one stock from another. Samples were machined from stock to standard dimensions 4.5-in. long by a 0.250-in. diameter 0.001-0.000.

Once machined, each sample was thoroughly degreased, numbered with a vibratool on each end next to the thread, and each end painted with the color code for that particular heat of material.

ACTUAL TESTING PROCEDURE

1. Allow proper warm up for electronic circuiting.
2. Set up cam on potentiometer to deliver proper voltage for desired thermal cycle.
3. Tighten cam and recheck peak and 180 second value.
4. Set microswitches at desired temperature.
   a. To initiate film on Midwestern oscillograph.
   b. To initiate load.

c. To initiate solenoid air valve.

d. To change current to cooling portion of the curve.

5. Place specimen on positioner and tighten knurled nuts to give correct free length and maintain the amount of specimen in jaws at a constant value.

6. Apply small preload to position, tighten specimen in jaws, provide good thermal and electrical contact between the jaws and the specimen.

7. Percussion-weld each wire of the chromel-alumel wire 0.010 in. thick to the specimen in the center of the free length keeping the wire perpendicular to the specimen approximately 1/16-in. apart.

8. Connect thermocouple to the circuitry.

9. Release preload to insure that breaking load is applied only at the desired temperature.

10. Give specimen low-temperature check run and observe current pattern on oscilloscope and Brush oscillograph. A uniform pattern of weld current would indicate proper thermocouple behavior. Whenever erratic firing patterns were observed, the thermocouple would be removed and replaced until a satisfactory pattern was observed.

11. The cam follower is now put over the actual testing can that will deliver the proper voltage for the desired thermal cycle. In Figure 6 the cam-potentiometer is shown with the cam follower at the end of a heating cycle.

12. Energize the cam follower; and circuitry will call for heat that the specimen will be heated and fractured at preset temperature.

13. Shut off cam follower which automatically releases load and electronic circuitry and repeat for more specimens.

ORNL-2571
Metallurgy and Ceramics
TID-4500 (13th ed., Rev.)
February 15, 1958

INTERNAL DISTRIBUTION

1. C. E. Center
2. Biology Library
3. Health Physics Library
4. Metallurgy Library
5-6. Central Research Library
7. Reactor Experimental Engineering Library
8-27. Laboratory Records Department
28. Laboratory Records, ORNL R.C.
29. A. M. Weinberg
30. L. B. Emlet (K-25)
31. J. P. Murray (Y-12)
32. J. A. Swartout
33. E. H. Taylor
34. E. D. Shipley
35. M. L. Nelson
36. W. H. Jordan
37. C. P. Keim
38. R. S. Livingston
39. R. R. Dickison
40. S. C. Lind
41. F. L. Culler
42. A. H. Snell
43. A. Hollaender
44. M. T. Kelley
45. K. Z. Morgan
46. J. A. Lane
47. A. S. Householder
48. C. S. Harrill
49. C. E. Winters
50. D. S. Billington
51. H. E. Seagren
52. D. Phillips
53. A. J. Miller
54. R. A. Charpie
55. C. F. Leitten
56. E. G. Bohlmann
57. M. J. Skinner
58. C. O. Smith
59. J. H. Frye, Jr.
60. W. W. Parkinson
61. W. D. Manly
62. J. E. Cunningham
63. G. M. Adamson, Jr.
64. J. W. Allen
65. R. J. Beaver
66. E. S. Bomar, Jr.
67. R. E. Clausing
68. J. H. Coobs
69. J. H. DeVan
70. L. M. Doney
71. D. A. Douglas, Jr.
72. E. A. Franco-Ferreira
73. R. J. Gray
74. J. P. Hammond
75. R. L. Heestand
76. T. Hikido
77-111. M. R. Hill
112. E. E. Hoffman
113. H. Inouye
114. L. K. Jetter
115. C. J. McHargue
116-120. P. Patriarca
121. M. L. Picklesimer
122. T. K. Roche
123. L. D. Schaeffer
124. G. P. Smith, Jr.
125. A. Taboada
126. W. C. Thurber
127. R. C. Waugh
128. H. L. Yakel, Jr.
129. J. H. Koenig (consultant)
130. H. Leidheiser, Jr. (consultant)
131. C. S. Smith (consultant)
132. H. A. Wilhelm (consultant)
133. ORNL - Y-12 Technical Library, Document Reference Section

EXTERNAL DISTRIBUTION

134. Division of Research and Development, AEC, ORO
135-144. Rensselaer Polytechnic Institute, Troy, N.Y.
145-634. Given distribution as shown in TID-4500 (13th ed., Rev.) under Metallurgy and Ceramics category